To the Graduate Council:

I am submitting herewith a thesis written by Marcus L. Simpson entitled "Evaluation and Development of the Instrumentation Used in the Measurement of Bone Piezoelectricity." I recommend that it be accepted in partial fulfillment of the requirements for the degree of Master of Science, with a major in Engineering Science.

Richard J. Jendrucko

R. J. Jendrucko, Major Professor

We have read this thesis and recommend its acceptance:

J. F. Wasserman

T. V. Bladek

Accepted for the Council:

L. Evans Peck

Vice Chancellor
Graduate Studies and Research

B

EVALUATION AND DEVELOPMENT OF THE INSTRUMENTATION USED IN THE MEASUREMENT OF BONE PIEZOELECTRICITY

A Thesis

Presented for the

Master of Science

Degree

The University of Tennessee, Knoxville

Marcus L. Simpson

August 1980

DEDICATION

This thesis is dedicated to my wife Nancy, whose loving support and understanding have made this academic achievement possible. It is with my deepest love and respect that this expression of gratitude is offered.

ACKNOWLEDGMENTS

The author is indebted to his advisor, Dr. R. J. Jendrucko, for his constant guidance and support. Special thanks is offered to Dr. J. F. Wasserman and Dr. T. V. Blalock for their invaluable contributions to this work.

Recognition is given to The University of Tennessee's Department of Engineering Science and Mechanics for their financial support and to Dr. A. Mathews and Dr. C. J. Remenyik for their assistance in a portion of the experimentation. Recognition is also extended to The University of Tennessee School of Dentistry for supplying some of the more important experimental materials.

Finally, a special note of appreciation is given to the Engineering Science and Mechanics shop personnel who unselfishly donated their time and talents throughout the duration of this research and without whom much of this work would not have been possible.

ABSTRACT

Inconsistencies in the data obtained from previous experimental investigations of the electrical properties of mechanically stressed bone have indicated the need for analysis and improvement of the measurement characteristics of the transduction systems used in such studies.

The current amplifier, which is introduced in this study for the measurement of bone piezoelectricity, was theoretically analyzed along with voltage and charge amplifiers similar to those used previously to determine the limitations of each device when measuring electrical signals from a high impedence source like bone. Experimental prototypes of voltage and current amplifers were then constructed and used to experimentally measure the electrical response obtained from small rectangular bars of dried human femur subjected to cantilever bending.

From both the theoretical and experimental analysis it was found that the speed of response of the voltage amplifier was severely limited by a high impedence source with a finite value of capacitance whereas the speed of response of the current amplifier was essentially independent of the value of source resistance. (The calculated value of rise time for the voltage amplifer was 4 milliseconds compared with 0.0171 milliseconds for the current amplifier.) From the experimental analysis it was also found that the magnitude of current obtained from stressed bone samples which had been dried using different techniques varied

considerably (3 to 35 picoamps), whereas the magnitude of voltage remained constant (30 millivolts), thus indicating that the current waveform may contain valuable information which had essentially been "integrated out" by the voltage amplifier.

Therefore, future studies of bone piezoelectricity should take into account the limitations of the transduction system and must provide for the measurement of both voltage and current to obtain a more complete understanding of this phenomena.

TABLE OF CONTENTS

CHAPTER PAGE

LIST OF FIGURES

FIGURE PAGE

CHAPTER I

INTRODUCTION

Since the 1800's man has recognized the importance of mechanical stress in the phenomena of bone remodeling. The first formal statement of this interaction was written by Julius Wolfe in 1892 and is currently recognized as Wolfe's Law: "The form of bone being given, the bone elements place and displace themselves in the direction of functional pressure and increase and decrease their mass to reflect the amount of functional pressure."[1] It was postulated that stress-induced changes in the cellular microenvironment of bone resulted in enzyme activation, pH changes, and/or orientation of macromolecules thus effecting cellular activity.[1] Current research indicates that it is the electric field produced by stressed bone which effects these changes in the cellular microenvironment, thus resulting in oriented bone growth.

Within the last two decades, considerable attention has been focused on the mechanisms regulating stress-induced bone remodeling. As a result two major research areas have developed involving: (1) measurement of electrical signals in bone for controlled stress-states in order to characterize the basic phenomena; and (2) stimulation of bone remodeling in intact animals and man by application of direct current in order to affect the course of clinical treatment of bone pathologies.

Many studies during the last eight years have demonstrated that electrical stimulation of bone growth is a viable clinical tool in

selected applications such as in the promotion of the healing of bony nonunions.[2] However, before such techniques can be used most effectively in the clinic on a routine basis, the effect as it occurs in nature should be thoroughly understood, thus necessitating a more quantitative approach than has been previously taken for the measurement of the electrical properties of mechanically stressed bone.

Within the framework of this need, the long term goal of the research presented here is to develop and evaluate improved transduction systems for the characterization of the electrical response in samples of stressed bone. As a first step, the present investigation has been focused on a theoretical characterization of the two major transduction systems reported in the literature, namely voltage and charge amplifiers. In addition, a new system, utilizing a current amplifier is studied. Finally, prototype current and voltage amplifiers are constructed and used to measure bone piezoelectric response in the laboratory. The time varying output of each device during mechanical loading is compared both theoretically and experimentally in order to elucidate the principal limitations of the measurement systems used so that a rational basis for the selection of an appropriate system can be made in future studies of bone piezoelectricity.

CHAPTER II

LITERATURE SURVEY

In this chapter, a review of the research which has been done on the measurement of bone piezoelectricity and the enhancement of bone remodeling by electrical stimulation is presented. Proposed mechanisms which are thought to be responsible for the development of bone piezoelectricity are briefly mentioned and the reader is referred to relevant reviews for further study. Finally a selected case history is discussed in order to show the viability of electrical enhancement of bone healing as a clinical tool.

I. EARLY WORK

The first discovery that bone generated an electrical signal in response to an applied stress was made by Yasuda in 1953.[3] Subsequently Yasuda and Fukada published a paper in 1957 showing that it was apparently classical piezoelectricity which was being demonstrated in stressed plates of human and ox femur.[4] The results of this study showed that not only was the electrical response directly proportional to the applied load (Direct Effect), but also when an electric field was applied, a mechanical strain was produced, the magnitude of which was directly proportional to the strength of the applied field (Converse Effect). Thus bone was found to behave similarly to well-known piezoelectric materials like quartz. It was also found that when the samples were cut at different orientations

relative to the principal (collagen) fiber axis, the polarity and magnitude of the response varied. A maximum response was obtained when the specimen was cut on an angle of 45° relative to the fiber axis which is also the point of maximum shear.[5] Thus it was concluded that the shearing stress in the collagen fibers caused the piezoelectric response in bone.

Similar observations were made in 1957 by Bassett who was apparently unaware of the earlier investigations of Yasuda and Fukada, but the results were interpreted as "artifact" due to the use of silver foil electrodes.[1] Later Bassett and Becker performed experiments using Ag-Cl eletrodes.[6] They measured the electrical response obtained when small bone strips, 30 × 2 × 1.2 mm, were subjected to bending loads and found that the concave aspect of the bent bone samples always became negative, while the convex aspect routinely became positive. Upon release of the load, a pulse of opposite polarity but of approximately equal magnitude was produced. Other investigators[7] reported stress potentials similar to those seen by Bassett and Becker, but occurring in bone from a variety of species and from a number of different anatomical sites. It was also found that different treatments such as oven drying (at up to 120°C), freezing and thawing, air drying, and boiling in water to cause protein denaturation or mineral leaching, did not markedly alter the electric response.[8] Thus, the conclusion was made that the phenomena of piezoelectricity was an inherent property of bone regardless of the biological state of the specimens used for the study.

II. RECENT WORK

Recent investigations have focused on refining loading techniques and standardizing such variables as temperature, humidity, and frequency of load applications so that a complete characterization of the electrical response in bone for a given stress can be made.

Initial investigations by Fukada and Yasuda used primarily a "lever mechanism" for the application of a compressive load.[4] Bassett and Becker applied a bending load by hanging weights from the end of their bone strips.[6] Currently small electromagnetic cells and larger hydraulic loading systems such as the Instron Testing Devices are being utilized in bone piezoelectric experiments for the application of both bending and compressive loads.[9,10] In addition to making the loads reproducible and minimizing vibrations, the load cells and hydraulic devices have the advantage of being able to change the frequency and characteristics of the driving signal. Thus the electrical response of bone to step, ramp, and sinusoidal loads applied at various frequencies can be conveniently studied.

Another variable which has received considerable attention in the literature is the effect of the moisture content of a given sample on the electrical response.[9,11-15] Initial studies of the electrical response of stressed bone were performed with dry specimens.[4,7,10,16,17] The question of whether the results of these experiments are applicable to the <u>in vivo</u> situation, where bone is hydrated, is extremely valid and as of yet, not fully answered. A variety of experimental techniques

have been used to study this question. Some investigators simply leave the specimens in a saline solution until equilibrium is reached, remove the specimens, blot off the excess moisture, and perform the experiments.[14] Others place the specimens in elaborately designed humidity chambers in order to perform the experiments.[11] Details of the experimental techniques and discrepancies in the results from these studies are discussed further in Chapter III.

In addition to moisture content, bone piezoelectricity has been found to be a function of temperature,[9] loading rate,[15] loading frequency,[9] geometry and specimen size,[5] and electrode placement.[5] Thus, it must be concluded that accurately defining the relationship between the stress applied to a bone specimen and the electrical response is an exceedingly complex process.

III. QUALITATIVE INTERPRETATIONS

A variety of mechanisms have been proposed for the electrical response of bone to an applied load and are well summarized and discussed in a review by Williams.[5] Thus, the various proposed mechanisms will only be listed here as follows:[18]

1. Distortion of H-bonds in collagen or its cross linkages;
2. Stress-sensitive p-n junctions;
3. Streaming potentials;
4. Stress reorientation of H_2O molecules;
5. Imperfections in the apatite mineral structure that would lower its symmetry;

6. Liberation of hydrogen ions by the rupture of cross linkages;
7. Alteration by stress of the spontaneous polarization of collagen.

Even though the importance of each mechanism is still very much subject to debate, Williams points out that in view of current research mechanisms (1) and (7) are the most likely to be of primary importance in bone.

IV. CLINICAL APPLICATIONS

A number of investigations by Bassett and Becker concentrated on the possible biological significance of piezoelectric effects in bone.[1,19,20] The earliest studies of these investigators focused on demonstrating that small electric fields could influence bone tissue remodeling phenomena at a microscopic level. Collagen molecules in solution were subjected to currents in the range of microamps and it was found that bonds of collagen formed at right angles to the electric field within one to five minutes.[1] Other studies showed distinct changes in electric fields surrounding regenerating amphibian limbs.[21] Thus, it was postulated that electrical stimulation might enhance bone growth. This theory was subsequently tested by implanting electrodes in dog femurs, in vivo, and applying electrical stimulation by means of a small battery pack.[1] After a period of several months, the femurs were histogically examined and it was discovered that a definite bone hypertrophy appeared at the cathode while there was atrophy noted at the anode.

Soon afterwards, electrical enhancement of bone growth was introduced in the clinical setting.[2] In a recent review by Jendrucko,[22] over 170 case studies in which electrical stimulation was used for the treatment of bone abnormalities are summarized. A most outstanding case was a 51-year-old woman who sustained a bimalleolar fracture of her right ankle. The fracture was immobilized for 13 weeks, then the patient was sent home. She returned one year later complaining of pain and swelling around her ankle and subsequent radiological examination revealed a bony nonunion at the fracture site. Electrical stimulation was applied to the fracture for a three month period. After three weeks of stimulation, the fracture was nonmobile and the tenderness had subsided. Radiographs at nine weeks revealed bony trabeculae crossing the previous defect, and at eleven weeks, the patient began full weight bearing. Thus, the enhancement of bone healing by electrical stimulation has been an alternative in cases where simple, traditional methods such as immobilization do not yield satisfactory long-term results.

CHAPTER III

RATIONALE

In the previous chapter, the two major fields of research being done in bone remodeling were discussed: (1) measurement of the electrical response in mechanically stressed bone and (2) enhancement of bone remodeling with electrical stimulation. In this chapter a negative feedback system is presented which hypothetically links these two fields. Arguments are then presented which show how the measurement of electrical signals in small bone samples can be clinically relevant. Major discrepancies in previously obtained experimental results are discussed thus pointing out the need for analysis and further development of the transduction systems which are being used to measure bone piezoelectricity. Finally the scope of this thesis is presented.

I. NEGATIVE FEEDBACK THEORY

As early as the nineteenth century, it was postulated that bone possesses a control system by which it remodels its architecture in a specific manner in response to mechanical stress.[1] Bassett has elaborated on this hypothesis and has proposed that bone remodeling is a negative feedback process in which the stresses are converted into one or more secondary signals which in turn orient new bone growth such that the stresses are minimized.[20] He concluded further that the signal is electrical in nature and that the stresses are converted into an electrical signal via the inherent piezoelectric properties of bone.

Then, through an unidentified mechanism, the electric signal influences the cellular activities of the osteoblasts such that oriented bone growth occurs. Hence, the two experimental observations that: (1) stressed bone produces an electric signal, and (2) electrical stimulation of bone enhances bone growth are linked. The phenomena of bone remodeling thus may be represented using modern control theory as is shown below in Figure 1. Here G_1, G_2, and H are transfer functions, F is the load which is applied to the bone, σ_1, is the local stress resulting from F, E is the electric response of the stressed bone, and σ_2, is the bone growth resulting from E.

The major focus of research in bone piezoelectricity has been to quantitatively define the transfer functions G_1 and G_2 in three dimensional space and time. The transfer function H, however, has been quantitatively defined only to the extent that it is now well known that negative polarization enhances bone growth while positive polarization results in bone destruction.[1] A variety of techniques for electrical stimulation of bone growth have been developed where currents ranging in magnitude from 1 to 40 microamps and in frequency from D.C. to 75 hertz have been applied.[22] Once the transfer functions G_1 and G_2 are accurately defined, though, the specific electric field needed for the treatment of a given bone fracture or abnormality can be computed and thus a systematic method for electrical enhancement of bone growth in the clinic can be developed. It must be noted here, however, that differences may exist in the transfer functions G_1 and G_2 for normal, physiological bone remodeling such as in the maintenance

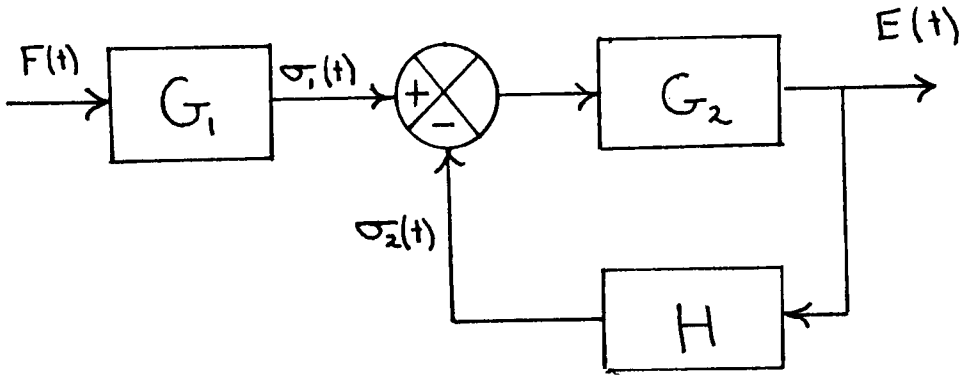

Figure 1. System Representation of Oriented Bone Growth.

of bone mass, and abnormal, pathological bone remodeling such as fracture healing. Thus there is much need for further research before an optimal clinical technique can be specified.

II. APPLYING BONE PIEZOELECTRICITY TO THE CLINICAL SETTING

The accurate determination of the transfer functions G_1 and G_2 is an extremely complicated process owing to the fact that bone is a nonuniform, anistropic, viscoelastic material. Thus, simply defining the stresses resulting from a given load in whole bone is a very significant undertaking. This task has been simplified somewhat in bone piezoelectric experiments by sectioning the whole bones into small regularly shaped cubes or bone strips. This technique permits uniform loading but complicates the measurement of the three dimensional electric field since the sample must be milled in precise orientations to obtain the stress-electric response relationship.

Using previously developed theory for piezoelectric materials, Fukada and Yasuda assumed that the electric field produced in stressed bone was of the form (direct effect neglecting counter polarization):[4]

$$P_i = d_{ij}\,\sigma_{ij} (i = 1,2,3;\ j = 1,2...6) \tag{1}$$

where the P_i are the components of the polarization vector which are linearly related to the stress σ_{ij} by the piezoelectric moduli, d_{ij}. Thus, by sectioning samples into small cubes at different orientations relative to the bone axis and applying compressive loads to opposite faces, known stresses σ_{ij} can be imposed. Then, by measuring the

electrical response in terms of electrical potential and relating the electrical potential to the polarization vector with the use of Maxwell's equations, the piezoelectric moduli can be calculated from Equation (1).

Difficulties arose when Cochran reported that in cantilever bending, the polarization voltage was not directly proportional to the stress.[15] He showed that the electric response does not increase as the cube of the thickness of the specimen as does the maximum fiber stress. Another observation made by Cochran which was not predicted by simple piezoelectric theory was that the magnitude of the electric response has been found to vary along the length of the beam. Thus, Williams has proposed an extension of the piezoelectric theory to include these findings.[5] He suggested that the polarization vector is not only a function of stress, but also of the stress gradient and thus is of the form:

$$P = d\sigma + f \frac{\partial \sigma}{\partial x} \tag{2}$$

where f is a fourth rank tensor which relates the stress gradient $\frac{\partial \sigma}{\partial x}$ to the polarization vector. For further study the reader is referred to a thesis by Breger[23] in which f is analyzed in detail for both cantilever and four point bending. Thus, once d and f are quantitatively determined by experiments with bone under compression and bending, the transfer functions G_1 and G_2 can be derived.

III. MAJOR EXPERIMENTAL DISCREPANCIES

There are three major experimental discrepancies which have appeared in the literature, all of which seem to be linked to the instrumentation used to make the measurements.

Measurements on Moist Bone

The first attempt to measure an electric response in moist collagen was made by Fukada and Yasuda in 1963 when they qualitatively observed that the piezoelectric effect was reduced as the moisture content of achilles tendon increased from 0 to 40%.[17] At that point the signal was so small that measurement was impractical. A similar finding was made by Marino and Becker when they also did a quantitative study using moist achilles tendon.[12] However, a difficulty was found in detecting the effect due to "charge leakage" in the sample, thus, they froze the specimens at -25°C in order to reduce the conductivity of the moist collagen. The same difficulty in measurement due to "charge leakage" was reported by Cochran et al. as they attempted to measure the electrical response of moist, decalcified bone.[15] Thus, the initial attempts to investigate the effect of moisture on bone piezoelectricity indicate a need for further development of the measurement systems.

Within the past ten years, only three major works have been published dealing with the effect of moisture on the piezoelectric constants in cortical bone. Anderson and Erickson reported that the d_{ij} coefficients in bovine femur increased as the moisture content

increased,[14] Reinish and Nowick, using human femur, reported that the d_{ij} coefficients decreased with increasing moisture content,[11] and Bur reported that the d_{12} and d_{13} coefficient of bovine femur increased as the relative humidity changed from 35 to 55% and decreased or remained constant from 75 to 98% relative humidity.[9] Thus, there is not only a difficulty in measuring piezoelectricity in moist bone, but also major discrepancies in quantitative results obtained to date.

Biphasic-Monophasic Signals

The "typical" electric response obtained from stressed bone is a biphasic signal which consists of an initial pulse upon application of the load, and a second pulse of approximately the same amplitude but opposite polarity upon release of the load as diagrammed in Figure 2.[6,7,8,13,15] The second or so-called "reverse pulse" is thought by several authors to be the result of measurement artifact.[16,18] This dispute is important because it may be that a biphasic signal is biologically insignificant whereas a monophasic pulse of duration less than a second can significantly alter such cellular parameters as pH.[19]

The proponents of the monophasic pulse have shown how variations in the input impedence of the amplifier measuring the phenomena affects the waveform obtained.[16] In this analysis bone was modeled as a voltage source having an impedence which was represented by a capacitor in parallel with a resistor (Figure 3). The transfer function was derived and the response to a step input was calculated. From the waveforms sketched in Figure 3 it can be concluded that if the input impedence

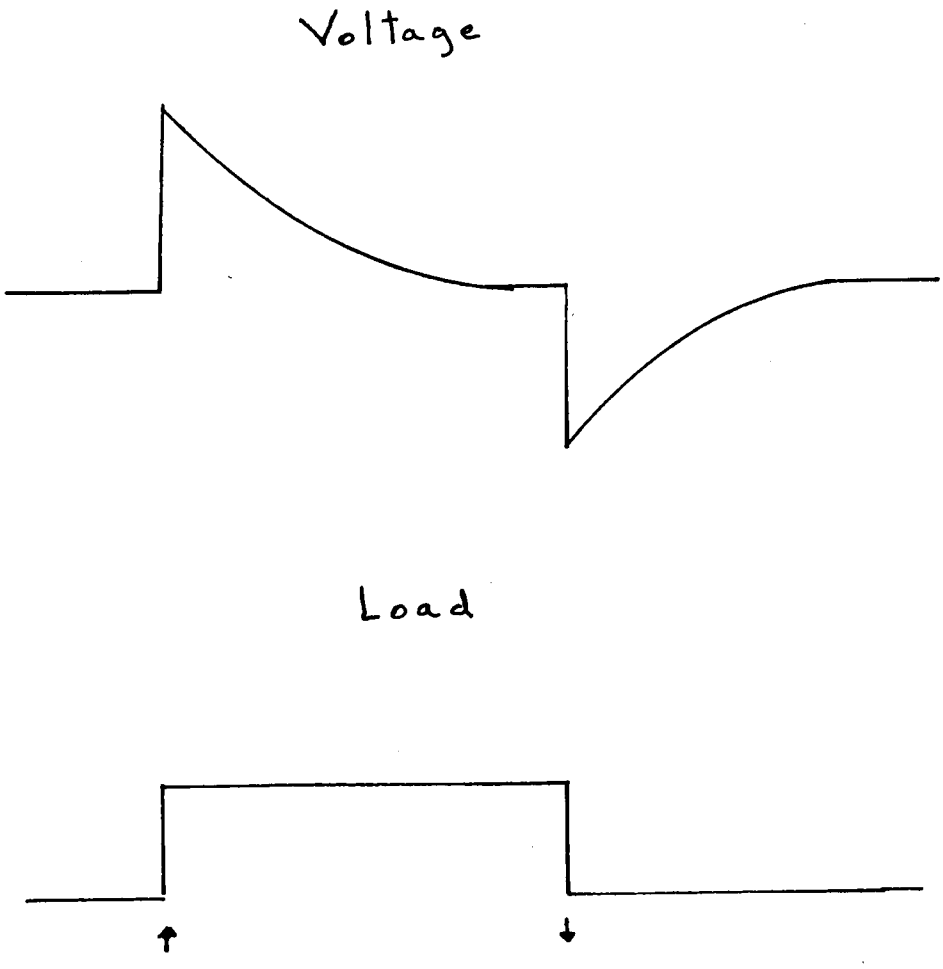

Figure 2. Typical Piezoelectric Waveform.

Model:

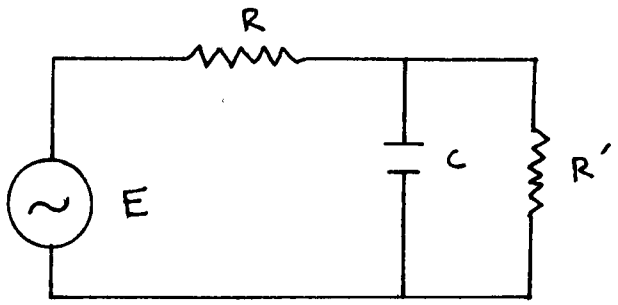

R = Resistance of Amplifier
R' = Resistance of Bone
C = Capacitance of Bone + Amplifier

Waveforms:

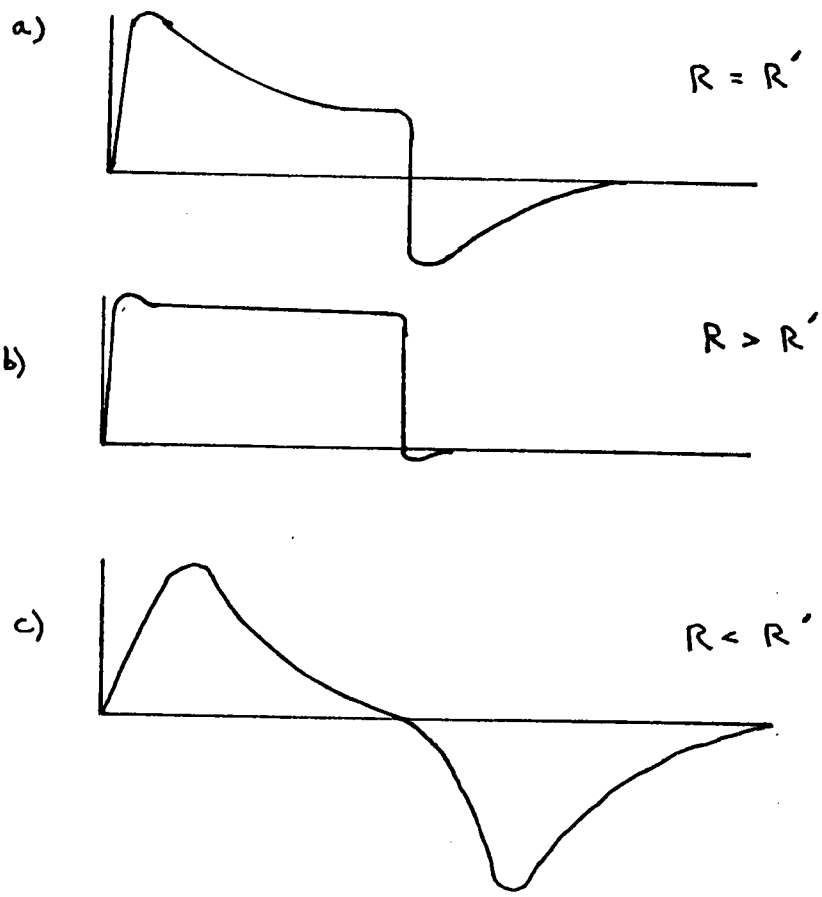

Figure 3. Bone Model and Response.

of the amplifier is much smaller than the resistance of the sample, the "typical" waveform is obtained. Williams reported experiment results which validate this analysis based on the fact that by increasing the impedence of a vibrating reed electrometer to 10^{16} ohms, a D.C. square wave was obtained for the bending of bone strips.[18] However, the highest reported value of bone resistance is 10^{12} ohms per cm,[16] and most investigators approximate the resistance of dry bone to be about 10^{9} ohms per cm.[7,24] Other studies[6,7] using amplifiers with input impedences well above these values report obtaining "typical" waveforms. Thus the actual waveform of the raw piezoelectric signal is still very much subject to debate.

Low Level D.C. Currents

Certain investigators have reported that frequently the initial electrical pulse occurring in stressed bone did not fully return to the base line.[6,8,13,15,18] Thus it has been postulated that stressed bone may produce low level D.C. currents. Bassett attributes this phenomena to one or more of the following: (1) slight changes in electrode position; (2) localized areas of high impedence; (3) temporary polarization of electrodes; or (4) viscoelastic changes within the bone.[15]

It is important to determine whether or not the slowly decaying potentials are "artifact" in order to more thoroughly understand the mechanisms acting normally in stress-controlled bone remodeling. For instance, if the true waveform is a pulse which returns to a neutral baseline, trigger mechanisms like enzymatic chain reactions should be

investigated, whereas if low level D.C. currents are present, mechanisms which alter cellular environment should be pursued. Thus, there is a need for further research into this phenomena.

IV. NEED FOR CURRENT AMPLIFICATION

The majority of investigators have used voltage amplifiers to measure the electrical response in stressed bone.[6-9,15,16,18,20,25] To date, a current amplifier has not been introduced for the measurement of bone piezoelectricity probably due to a general lack of knowledge of current amplification techniques. It is of interest to note that two studies have been performed with charge amplifiers,[10,11] which, like the current amplifiers, provide a low impedence pathway for the signal. However, the charge amplifier integrates the current, thus losing the ability to display the actual waveform.

By using current amplification the two questions: (1) whether or not low level D.C. currents are produced by stressed bone and (2) whether the signal is biphasic or monophasic would be conveniently answered. This follows because low level D.C. currents down to the level of fempto amps are detectable by state of the art current amplifiers. Also, if the second pulse is not an artifact, reverse currents would be present and would be detectable by current amplification. In addition to answering these questions, the use of a current amplifier would eliminate the problem of charge leakage in moist bone because it provides a much lower impedence pathway for the signal than the bone sample itself. Therefore, the charge would "leak" through the amplifier

rather than through the sample, and thus a much more meaningful quantitative result could be obtained from moist bone using current amplification as opposed to voltage amplification. Hence it is hoped that the development of this new transduction system will contribute to the existing body of literature on bone piezoelectricity.

V. SCOPE OF THESIS

Within the framework of the needs presented in this chapter, the goals of this thesis are as follows:

1. To theoretically compare the operational characteristics of voltage, charge, and current amplifiers with respect to transfer functions, stability, and noise, assuming bone as the signal source.

2. To develop a transduction system to detect and amplify either current or voltage.

3. To experimentally compare the voltage and current waveforms obtained from bending small strips of dry cortical bone.

CHAPTER IV

THEORY AND DESIGN CONSIDERATIONS

In this chapter, the transfer functions for voltage, current, and charge amplifiers are derived assuming that bone is the signal source. These transfer functions are then used to examine the stability of each amplifier when measuring the electrical response of mechanically stressed bone that has been hydrated to various degrees. Finally, noise equations are generated to determine minimum signal levels which are detectable by each amplifier.

I. DERIVATION OF TRANSFER FUNCTION

The electrical modeling of bone was investigated by Stephan, Swansen, and Mueller who determined that bone behaves electrically like a resistor in parallel with a capacitor.[24] Thus, in this analysis, mechanically stressed bone tissue was assumed to be a signal source which has a complex impedence represented by a resistor in parallel with a capacitor. In addition, a voltage source and a current source are theoretically interchangeable since a Norton current source can be represented by its Thevenin equivalent voltage source and vice versa, therefore, bone was assumed to be a current source for all amplifiers in order to simplify the analysis.

The schematic of a general, nonideal, linear amplifier can be represented as shown in Figure 4.[26] In this model and in accordance with standard nomenclature, R_1 and C_1 are the input resistance and

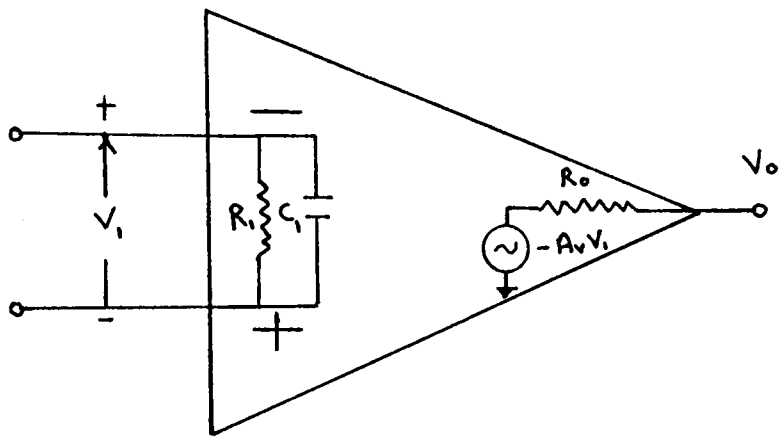

Figure 4. General Op Amp Model.

capacitance respectively, R_o is the output resistance, V_1 is the differential input voltage and A_v is the open loop gain. The amplifier is assumed to be a single pole system,[26] thus:

$$A_v = \frac{A_o}{1 + s/\omega_o} \tag{3}$$

In this equation, A_o is the magnitude of the open loop gain, and ω_o is the -3dB radian frequency associated with the pole.

Voltage Amplifier

The model used in this analysis for the derivation of the voltage amplifier transfer function is shown in Figure 5.[26] In this figure R_g and C_g are the source resistance and capacitance respectively, R_B is the bias resistor, R_2 and R_3 are the feedback resistors, and R_L is the load resistance. Letting Z_g represent R_g in parallel with C_g and letting Z_1 represent R_1 in parallel with C_1, the nodal equations are obtained by inspection as follows:

$$I_1 = V_1\left(\frac{1}{Z_g} + \frac{1}{R_B} + \frac{1}{Z_1}\right) + V_2\left(-\frac{1}{Z_1}\right)$$

$$0 = V_1\left(-\frac{1}{Z_1}\right) + V_2\left(\frac{1}{Z_1} + \frac{1}{R_2} + \frac{1}{R_3}\right) + V_o\left(-\frac{1}{R_3}\right)$$

$$0 = V_1\left(-\frac{A_v}{R_o}\right) + V_2\left(\frac{A_v}{R_o} - \frac{1}{R_3}\right) + V_o\left(\frac{1}{R_o} + \frac{1}{R_L} + \frac{1}{R_3}\right) \tag{4}$$

This set of equations represents three simultaneous equations and three unknowns (V_1, V_2, and V_o) which are put into standard matrix form in order to obtain a solution, thus:

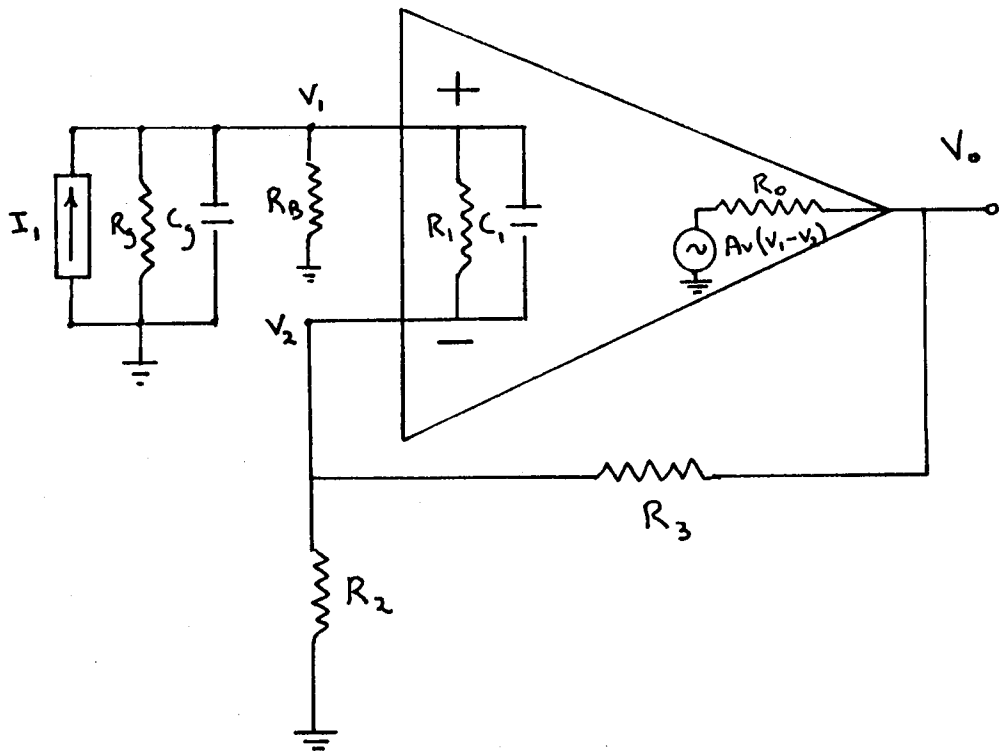

Figure 5. Voltage Amplifier.

$$\begin{bmatrix} I_1 \\ 0 \\ 0 \end{bmatrix} = \begin{bmatrix} \left(\frac{1}{Z_g} + \frac{1}{R_B} + \frac{1}{Z_1}\right) & \left(-\frac{1}{Z_1}\right) & 0 \\ \left(-\frac{1}{Z_1}\right) & \left(\frac{1}{Z_1} + \frac{1}{R_2} + \frac{1}{R_3}\right) & \left(-\frac{1}{R_3}\right) \\ \left(-\frac{A_v}{R_o}\right) & \left(\frac{A_v}{R_o} - \frac{1}{R_3}\right) & \left(\frac{1}{R_o} + \frac{1}{R_L} + \frac{1}{R_3}\right) \end{bmatrix} \begin{bmatrix} V_1 \\ V_2 \\ V_o \end{bmatrix} \tag{5}$$

The transfer function $\frac{V_o}{I_1}$ can now be derived by applying Kramer's rule for the solution of simultaneous equations. Thus the transfer function becomes:

$$\frac{V_o}{I_1} = \frac{\frac{A_v}{R_o}\left(\frac{1}{Z_1} + \frac{1}{R_2} + \frac{1}{R_3}\right) - \frac{1}{Z_1}\left(\frac{A_v}{R_o} - \frac{1}{R_3}\right)}{\left(\frac{1}{Z_g} + \frac{1}{R_B} + \frac{1}{Z_1}\right)\left[\left(\frac{1}{Z_1} + \frac{1}{R_2} + \frac{1}{R_3}\right)\left(\frac{1}{R_o} + \frac{1}{R_L} + \frac{1}{R_3}\right)\right.} \\ \left. + \frac{1}{R_3}\left(\frac{A_v}{R_o} - \frac{1}{R_3}\right)\right] - \frac{1}{Z_1}\left[\frac{1}{Z_1}\left(\frac{1}{R_o} + \frac{1}{R_L} + \frac{1}{R_3}\right) + \frac{A_v}{3R_o}\right] \tag{6}$$

Since Z_g and Z_1 represent parallel combinations of resistors and capacitors, the following substitutions can be made:

$$\frac{1}{Z_g} = \frac{1}{R_g} + s\ C_g \tag{7}$$

$$\frac{1}{Z_1} = \frac{1}{R_1} + s\ C_1 \tag{8}$$

Substituting Equations (3), (7), and (8) into Equation (6), the general transfer function is obtained as follows:

$$\frac{V_o}{I_1} = \frac{s^2\left[\frac{C_1 R_o}{A_o \omega_o R_3}\right] + s\left[\frac{R_o}{A_o \omega_o R_1 R_3} + \frac{C_1 R_o}{A_o R_3}\right] + \left[\frac{1}{R_2} + \frac{1}{R_3} + \frac{R_o}{A_o R_1 R_3}\right]}{s^3\left[\frac{C_g C_1}{A_o \omega_o}\left(1 + \frac{R_o}{R_L} + \frac{R_o}{R_3}\right)\right] + s^2\left[\frac{C_1}{A_o \omega_o}\left(\left(\frac{1}{R_g} + \frac{1}{R_B}\right)\left(1 + \frac{R_o}{R_L} + \frac{R_o}{R_3}\right)\right.\right.}$$

$$\left.\left. + \left(\frac{1}{R_2} + \frac{1}{R_3}\right)\left(1 + \frac{R_o}{R_L} + \frac{R_o}{R_3}\right)\right)\right.$$

$$+ \frac{C_g}{A_o \omega_o}\left(\frac{1}{R_2} + \frac{1}{R_3} + \frac{1}{R_1} + C_1 \omega_o\right)\left(1 + \frac{R_o}{R_L} + \frac{R_o}{R_3}\right)$$

$$\left. - \frac{\left(C_g + C_1\right) R_o}{A_o \omega_o R_3^2}\right] s\left[\frac{1}{A_o \omega_o R_1}\left(\frac{1}{R_2} + \frac{1}{R_3}\right)\left(1 + \frac{R_o}{R_L} + \frac{R_o}{R_3}\right)\right.$$

$$+ \frac{1}{A_o \omega_o}\left(\frac{1}{R_g} + \frac{1}{R_B}\right)\left(\frac{1}{R_2} + \frac{1}{R_3} + \frac{1}{R_1} + C_1 \omega_o\right)\left(1 + \frac{R_o}{R_L} + \frac{R_o}{R_3}\right)$$

$$- \left(\frac{1}{R_g} + \frac{1}{R_B} + \frac{1}{R_1}\right)\left(\frac{R_o}{A_o \omega_o R_3^2}\right) + \frac{C_1}{A_o}\left(\frac{1}{R_2} + \frac{1}{R_3}\right)\left(1 + \frac{R_o}{R_L} + \frac{R_o}{R_3}\right)$$

$$\left. + \frac{C_g}{A_o}\left(\frac{1}{R_2} + \frac{1}{R_3} + \frac{1}{R_1}\right)\left(1 + \frac{R_o}{R_L} + \frac{R_o}{R_3}\right) + \frac{C_g}{R_3} - \frac{R_o\left(C_g + C_1\right)}{A_o R_3^2}\right]$$

$$+ \left[\frac{1}{A_o R_1}\left(\frac{1}{R_2} + \frac{1}{R_3}\right)\left(1 + \frac{R_o}{R_L} + \frac{R_o}{R_3}\right)\right.$$

$$+ \frac{1}{A_o}\left(\frac{1}{R_g} + \frac{1}{R_B}\right)\left(\frac{1}{R_2} + \frac{1}{R_3} + \frac{1}{R_1}\right) \cdot \left(1 + \frac{R_o}{R_L} + \frac{R_o}{R_3}\right)$$

$$\left. + \frac{1}{R_3}\left(\frac{1}{R_g} + \frac{1}{R_B}\right) - \frac{R_o}{A_o R_3^2}\left(\frac{1}{R_g} + \frac{1}{R_B} + \frac{1}{R_1}\right)\right] \qquad (9)$$

For the typical op amp it can be assumed that R_1, R_2, R_3, R_g, R_B and R_L is much greater than R_o, and also that the open loop gain A_o is large,[26] thus:

$$R_1,\ R_2,\ R_3,\ R_g,\ R_B,\ R_L \gg R_o \tag{10}$$

$$A_o \gg 1 \tag{11}$$

Since the input capacitance of an op amp is in the range of picofarads, and since bone has been reported to have a capacitance as large as microfarads,[24] it can also be assumed that:

$$C_g \gg C_1 \tag{12}$$

Using the preceding assumptions, Equations (10), (11), and (12), Equation (9) can be simplified to obtain

$$\frac{V_o}{I_1} = \frac{\dfrac{R_2 + R_3}{R_2}\left(\dfrac{R_g R_B}{R_g + R_B}\right)}{s^3\left[\dfrac{R_3 C_g C_1 R_g R_B}{A_o \omega_o (R_g + R_B)}\right] + s^2\left[\dfrac{C_g R_3 R_B R_g}{A_o \omega_o (R_g + R_B)}\left(\dfrac{1}{R_2} + \dfrac{1}{R_3} + \dfrac{1}{R_1} + C_1 \omega_o\right)\right]}$$

$$+ s\left[\left(\frac{1}{R_2} + \frac{1}{R_3} + \frac{1}{R_1}\right)\frac{R_3}{A_o \omega_o} + \frac{R_3 R_g R_B\left(\dfrac{1}{R_2} + \dfrac{1}{R_3}\right)}{R_1 A_o \omega_o (R_g + R_B)} + \frac{C_g R_g R_B}{R_g + R_B}\right] + 1 \tag{13}$$

Current Amplifier

The model used in this analysis to derive the transfer function for the current amplifier is shown in Figure 6. Since the current and charge amplifiers are similar with the difference that the charge amplifier contains a shunt capacitor C_f in the feedback loop,[26] Figure 6 will also be used in the analysis of the charge amplifier.

Using nodal analysis, two simultaneous equations involving two unknowns (V_1 and V_o) can be written by inspection from Figure 6.

$$I_1 = V_1\left(\frac{1}{Z_g} + \frac{1}{R_f} + \frac{1}{Z_1}\right) + V_o\left(-\frac{1}{R_f}\right)$$

$$0 = V_1\left(\frac{A_v}{R_o} - \frac{1}{R_f}\right) + V_o\left(\frac{1}{R_o} + \frac{1}{R_f} + \frac{1}{R_L}\right) \qquad (14)$$

The transfer function $\frac{V_o}{I_1}$ was obtained using Kramer's rule as before, and the same assumptions, Equations (10), (11), and (12), were made to reduce the transfer function to a usable form. Thus, for the current amplifier, the final form of the transfer function is:

$$\frac{V_o}{I_1} = \frac{\frac{R_o}{C_g R_f}\left(s - \frac{A_o \omega_o R_f}{R_o}\right)}{s^2 + s\left[\omega_o + \frac{1}{R_f C_g} + \frac{1}{R_1 C_g}\right] + \frac{A_o \omega_o}{R_f C_g}} \qquad (15)$$

This equation is similar in form to one obtained from an analysis performed by Kennedy, who also derived the transfer function of a current amplifier assuming a current signal source with a complex impedence.[27]

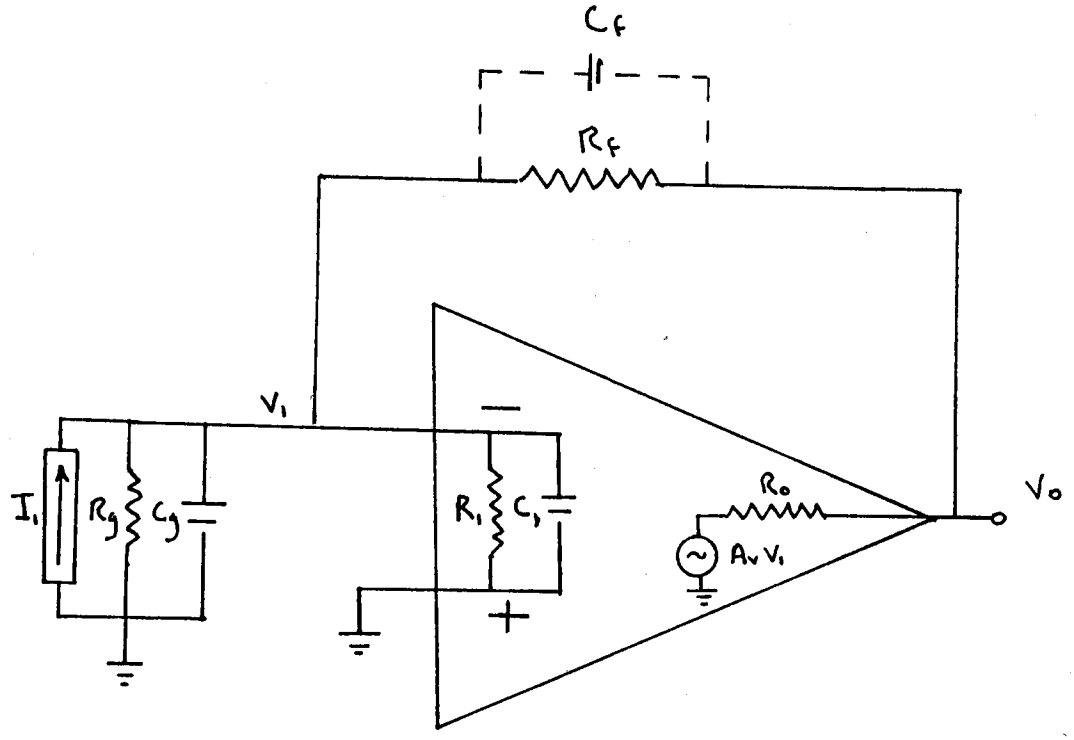

Figure 6. General Model of the Current and Charge Amplifiers.

Charge Amplifier

As discussed above, the charge amplifier is essentially a current amplifier with a shunt capacitor in the feedback path. Thus, including the feedback capacitor in the analysis, the nodal equations are obtained as follows:

$$I_1 = V_1\left(\frac{1}{Z_g} + \frac{1}{Z_f} + \frac{1}{Z_1}\right) + V_o\left(-\frac{1}{Z_f}\right)$$

$$0 = V_1\left(\frac{A_v}{R_o} - \frac{1}{Z_f}\right) + V_o\left(\frac{1}{R_o} + \frac{1}{Z_f} + \frac{1}{R_L}\right) \tag{16}$$

Where Z_f is the parallel combination of R_f and C_f. In a charge amplifier, the capacitor C_f is assumed to be large enough such that:[27]

$$\frac{1}{R_f C_f} << \omega_o \tag{17}$$

Using this assumption and Equations (10), (11), and (12), the transfer function was derived and simplified as before, yielding for the charge amplifier:

$$\frac{V_o}{I_1} = \frac{-R_f}{s^2\left[\frac{R_f(C_f + C_g)}{A_o\omega_o}\right] + s\left[R_f\left(C_f + \frac{C_g}{A_o}\right)\right] + 1} \tag{18}$$

This result also agrees with Kennedy's findings for the case of a charge amplifier driven by a current source with a complex impedence.

II. STABILITY ANALYSIS

The transfer functions presented above are of the general form,

$$F(s) = \frac{es^3 + fs^2 + gs + h}{as^3 + bs^2 + cs + d} \tag{19}$$

If a step function $\left(\frac{1}{s}\right)$ is applied to the transduction system, the output would be $\left(\frac{1}{s}\right) F(s)$ or

$$G(s) = \frac{es^3 + fs^2 + gs + h}{as^4 + bs^3 + cs^2 + ds} \tag{20}$$

Defining the roots of the characteristic equation as

$$as^4 + bs^3 + cs^2 + ds = s(s - r_1)\ (s - r_2)\ (s - r_3), \tag{21}$$

the general Equation (20) can be factored into the following form using partial fractions:

$$G(s) = \frac{\alpha}{s} + \frac{\beta}{s - r_1} + \frac{\gamma}{s - r_2} + \frac{\delta}{s - r_3} \tag{22}$$

where,

$$\alpha = - \frac{h}{r_1 r_2 r_3} \quad , \tag{23}$$

$$\beta = \frac{er_1^3 + fr_1^2 + gr_1 + h}{r_1(r_1 - r_2)(r_1 - r_3)} \tag{24}$$

$$\gamma = \frac{er_2^3 + fr_2^2 + gr_2 + h}{r_3(r_2 - r_1)(r_2 - r_3)} \tag{25}$$

$$\delta = \frac{er_3^3 + fr_3^2 + gr_3 + h}{r_3(r_3 - r_1)(r_3 - r_2)} \tag{26}$$

By taking the inverse Laplacian of Equation (22), the transient response is obtained, thus:

$$G(t) = \alpha + \beta e^{r_1 t} + \gamma e^{r_2 t} + \delta e^{r_3 t} \tag{27}$$

There are three cases which need to be examined:

1. If all of the roots are zero, then the coefficients α, β, γ, and δ go to infinity and the transient response would theoretically increase without bounds.

2. If the real part of the root is positive, then e^{rt} goes to $e^{+\infty}$ again indicating instability.

3. If the real part of the root is negative, e^{-rt} would approach $e^{-\infty}$ or zero, therefore the transient response would be damped and thus the system would be stable.

Hence, by finding under what conditions the roots of the characteristic equation are zero, positive, or negative, the stability of the system can be determined.

In this analysis, since the impedence of bone is a function of moisture content (the dielectric constant of water is larger than that of air), the stability of each amplifier was examined for both moist and dry bone experiments by using selected values of R_g and C_g. These

values were substituted into the characteristic equation of each amplifier and the respective roots were determined by using a standard I.M.S.L. computer routine for the solution of polynomials (U.T. Computer Center). The results and conclusions of the stability analysis are presented below in Chapter VI.

III. NOISE ANALYSIS

The intent of performing the noise analysis was to obtain an order of magnitude approximation of the minimum signal level which can be detected in bone with a specific amplifier. Thus only "white noise" was examined.

Voltage Amplifier

The model which was used for the noise analysis of the voltage amplifier is shown in Figure 7.[28] In this figure $\overline{E_g^2}$, $\overline{E_{R2}^2}$, and $\overline{E_{R3}^2}$ represent the thermal noise generated by each resistor, and $\overline{E_n^2}$ and $\overline{I_n^2}$ represent the equivalent noise voltage and current respectively, which are generated by the amplifier. Defining the noise power spectral density as $N(\omega)$ and the transfer function from the noise source to the output as $T(j\omega)$, the equivalent output noise, $\overline{E_{no}^2}$, can be written as follows:[28]

$$\overline{E_{no}^2} = \int_o^\infty N(\omega)T(j\omega)T(-j\omega)\frac{\partial\omega}{2\pi} \tag{28}$$

There are two types of noise sources which are depicted in Figure 7:

1. Thermal noise from the resistors;
2. Equivalent noise from the amplifier.

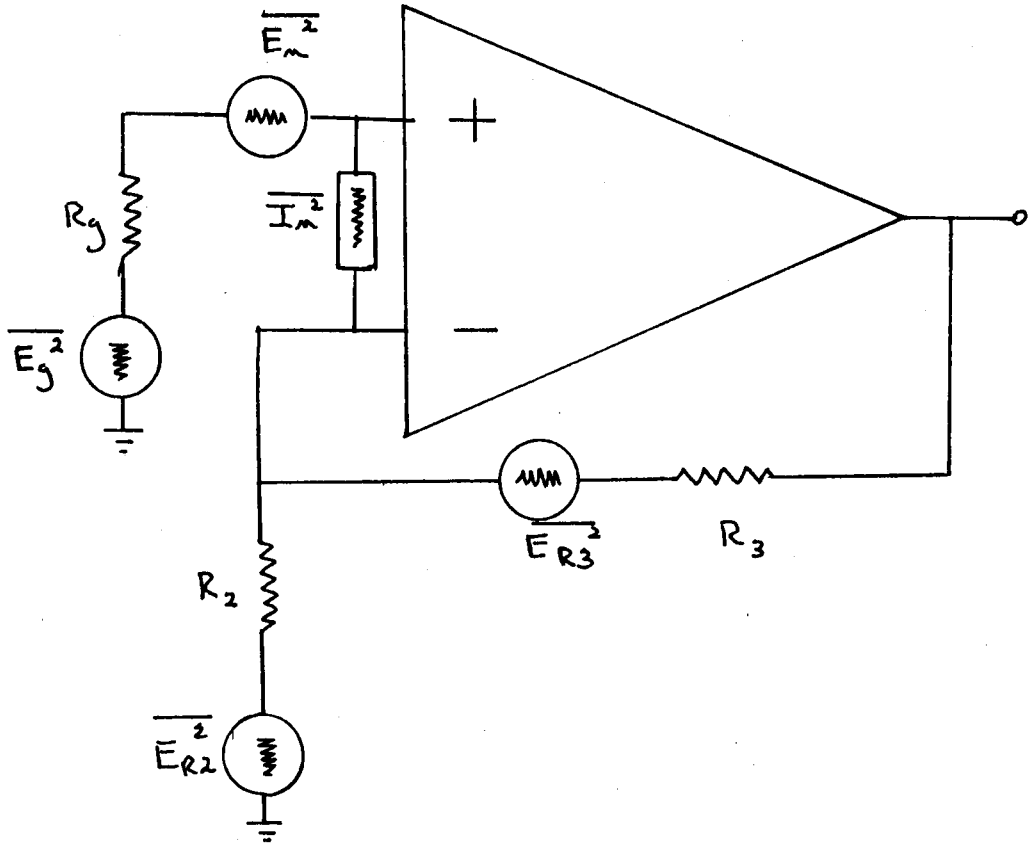

Figure 7. Noise Model of the Voltage Amplifier.

The noise power spectral density for thermal noise is given by:[28]

$$N(\omega)_T = 4KTR \tag{29}$$

In this equation K is Boltzman's constant, T is the absolute temperature, and R is the value of the resistor. Combining Equations (28) and (29), the contribution to the output noise due to thermal effects can be obtained as:

$$E_{noT}^2 = 4KTRA^2 (f_2 - f_1) \tag{30}$$

Since by definition "white noise" has no frequency dependence, the transfer function, $T(j\omega)$, was assumed to be a constant, A, in the region of "white noise," $f_1 < f < f_2$.

The contributions to the output noise from the equivalent input noise voltage and current respectively are given by Equations (31) and (32):[29]

$$\overline{E_{noV}^2} = \overline{E_n^2} B^2 (f_2 - f_1) \tag{31}$$

and

$$\overline{E_{noI}^2} = \overline{I_n^2} C^2 (f_2 - f_1) \tag{32}$$

In these equations B and C represent constant noise power transfer functions in the region of "white noise."

After the contribution from each source was analyzed at the output, the contributions were quadratically summed to obtain the total equivalent output noise. This value was then divided by the noise power transfer function of the amplifier to obtain the equivalent input noise of the system. The square root of the input noise in turn represents the order of magnitude of the smallest detectable signal. Thus, for the voltage amplifier depicted in Figure 7, the total output noise voltage can be written as follows:

$$\frac{\overline{E_{no}^2}}{(f_2 - f_1)} = \overline{E_n^2}\left(\frac{R_3 + R_2}{R_2}\right)^2 + \overline{I_n^2}\left(R_3\right)^2 + \overline{E_g^2}\left(\frac{R_3 + R_2}{R_2}\right)^2 + \overline{E_{R_2}^2}\left(\frac{R_3}{R_2}\right)^2 + \overline{E_{R_3}^2} \tag{33}$$

Substituting in Equation (30) for thermal noise, dividing by the noise power transfer function of the amplifier $\left(\frac{R_3 + R_2}{R_2}\right)^2$, and simplifying the equation for the total equivalent input noise for a voltage amplifier is obtained as follows:

$$\frac{\overline{E_{ni}^2}}{(f_2 - f_1)} = \overline{E_n^2} + \overline{I_n^2}\left(\frac{R_2R_3}{R_2 + R_3}\right)^2 + 4KT\left[R_g + R_2\left(\frac{R_3}{R_3 + R_2}\right)^2 + R_3\left(\frac{R_2}{R_3 + R_2}\right)^2\right] \tag{34}$$

Current and Charge Amplifiers

The model used in the noise analysis of the current and charge amplifiers is shown in Figure 8.[28] Since only the thermal noise generated by the resistive components, and the equivalent noise generated by the amplifier are considered in this analysis, the charge amplifier has the same equivalent input noise as the current amplifier. Following the same reasoning used for the voltage amplifier, the total output noise was derived for the current amplifier, and may be expressed as follows:

$$\frac{\overline{E_{no}^2}}{(f_2 - f_1)} = \overline{E_g^2}\left(\frac{R_f}{R_g}\right)^2 + \overline{E_n^2}\left(\frac{R_f + R_g}{R_g}\right) + \overline{I_n^2}\left(R_f\right)^2 + \overline{E_{R_f}^2} \qquad (35)$$

Simplifying this expression as before, and dividing by the noise power transfer function of the current amplifier, $\left(\frac{R_f}{R_g}\right)^2$, the equation of the equivalent input noise is obtained as follows:

$$\frac{\overline{E_{ni}^2}}{(f_2 - f_1)} = \overline{E_n^2}\left(\frac{R_f + R_g}{R_f}\right) + \overline{I_n^2}\, R_g^2 + 4KT\left(R_g + R_f\left(\frac{R_g}{R_f}\right)^2\right) \qquad (36)$$

The results of the noise analysis are presented below in Chapter VI, where Equations (34) and (36) are used to estimate the minimum electric response which can be detected in mechanically stressed bone with the voltage and current amplifiers utilized in the experiments described here.

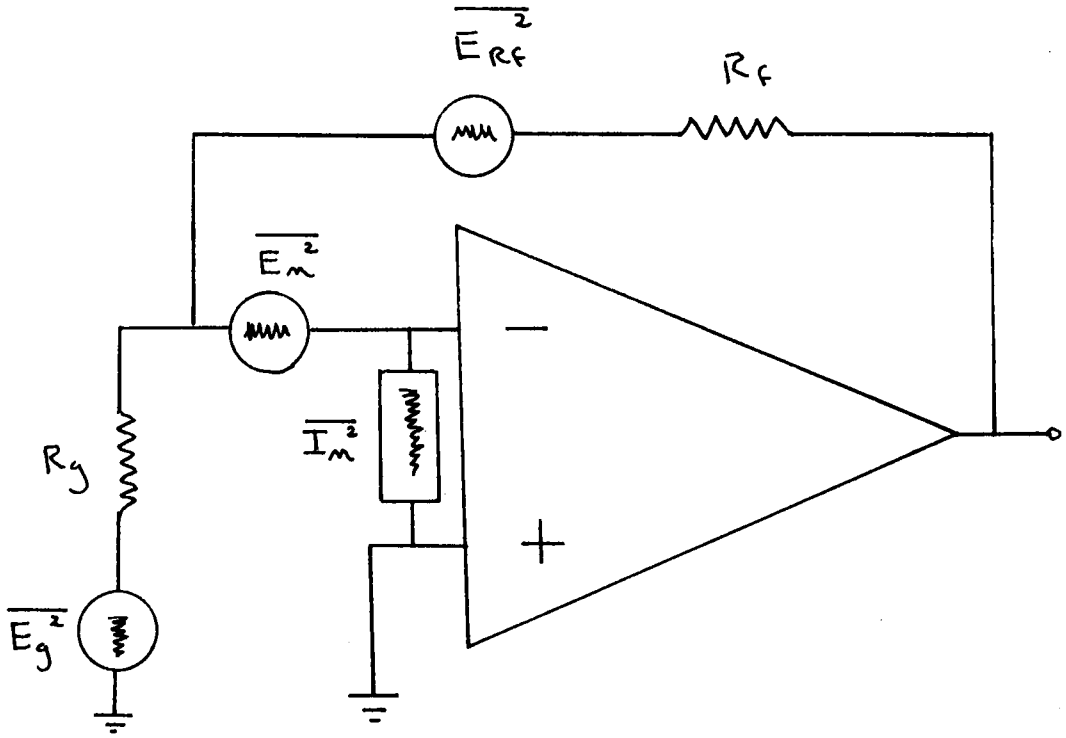

Figure 8. Noise Model of the Current and Charge Amplifiers.

IV. RISE TIME

The rise time is an indicator of how fast a signal a given amplifier will accept. It is calculated from the bandwidth of the closed loop response and is given by Equation (37):[26]

$$\tau_r = \frac{0.35}{f_{hi}} \tag{37}$$

where f_{hi} is the -3dB frequency which can be approximated by dividing the gain bandwidth product of the amplifier by the closed loop gain of the amplifier. Limitations of this approximation are discussed below in Chapter VI.

CHAPTER V

EXPERIMENTAL DESIGN

In this chapter, the theory developed in Chapter IV is used to design a transduction system which measures either current or voltage in stressed bone. The technique utilized in preparing the bone specimens for experimentation is then discussed. Finally, the experimental protocol for the direct measurement of the electric response in mechanically stressed bone is presented.

I. INSTRUMENTATION

The importance of the input impedence of a voltage amplifier in determining the measurement accuracy was pointed out by Shamos and Lavine.[16] It was concluded in their analysis that an accurate measurement could only be obtained if the input impedence of the amplifier was much greater than the bone source impedence. This conclusion can be reached by examining Equation (13) for a D.C. input signal:

$$V_0 = I_1 R_g \left(\frac{R_2 + R_3}{R_2}\right)\left(\frac{R_B}{R_g + R_B}\right) \tag{38}$$

Thus, if $R_B >> R_g$, the term $\frac{R_B}{R_g + R_B}$ is approximately equal to one and the signal is not attenuated by voltage division. Since the impedence of dry bone is approximately 10^9 ohms, the input impedence of the voltage amplifier should therefore be at least 10^{11} ohms to obtain less than 1% attenuation.

For the current amplifier, the sensitivity is determined by the magnitude of the feedback resistor R_f as can be seen from examining Equation (15) for a D.C. input:

$$V_0 = -I_1 R_f \tag{39}$$

A complication arises in that resistors above 10^9 ohms are difficult to fabricate and tend to exhibit an unstable resistance value, thus restricting the magnitude of current which can be measured. To circumvent this problem, the "T configuration" that is depicted in Figure 9 can be used which in essence increases the effective feedback resistance by $\frac{R_2 + R_1}{R_1}$ assuming $R_f >> R_1, R_2$.[25] Thus, the major limiting factor in the measurement of low level currents is the noise produced by the amplifier. Since the magnitude of current generated in stressed bone has not been reported, a high quality, low noise electrometer op amp, the AD515, was selected for use in these experiments. Additional benefits of this device are:

1. High input impedence (10^{13} ohms);
2. Low cost ($16.00);
3. Availability;
4. Low offset voltage and temperature drift;
5. External null offset to neutralize any electrode polarization.

The manufacturer's specifications for the AD515 amplifier are listed in Table 1. Also, due to the lack of knowledge about the current generated in stressed bone, the value of R_f had to be determined experimentally. The optimum value of R_f considering rise time, noise, and stability was found to be 10^9 ohms.

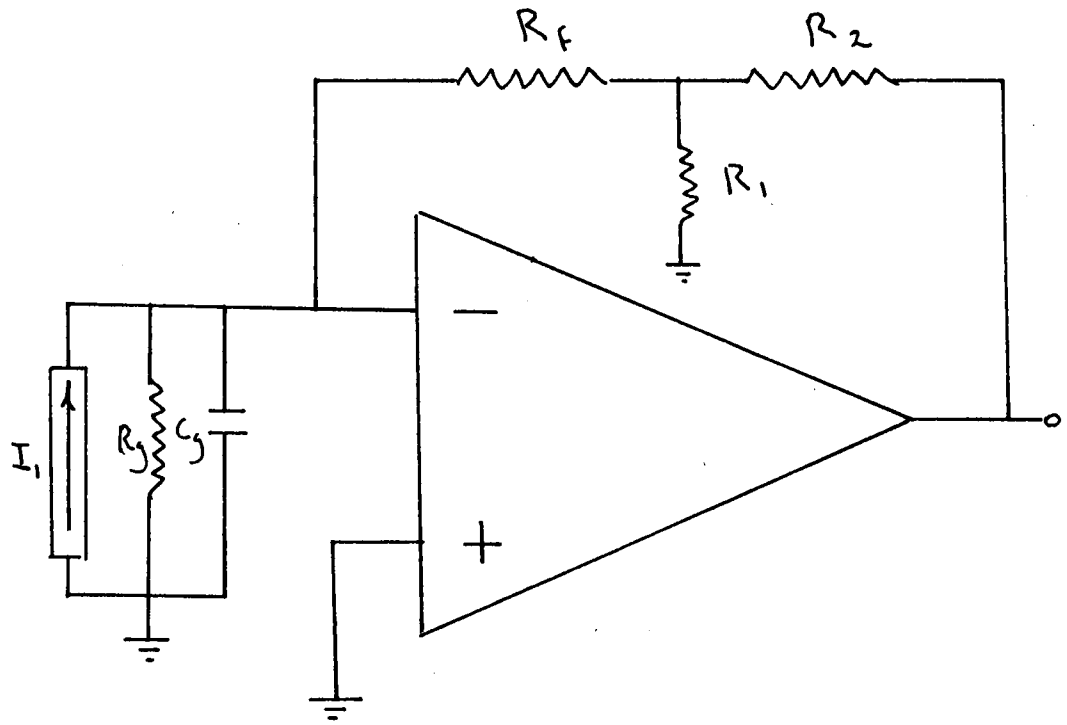

Figure 9. "T" Configuration for Increasing Effective Feedback Resistance.

Table 1. Manufacturer's Specifications for the AD515.

MODEL	AD515J
OPEN LOOP GAIN (Note 1)	
V_{out} = ±10V, $R_L \geq 2k\Omega$	20,000V/V min
$R_L \geq 10k\Omega$	40,000V/V min
T_A = min to max $R_L \geq 2k\Omega$	15,000V/V min
OUTPUT CHARACTERISTICS	
Voltage @ R_L = 2kΩ, T_A = min to max	±10V min (±12V typ)
@ R_L = 10kΩ, T_A = min to max	±12V min (±13V typ)
Load Capacitance (Note 2)	1000pF
Short Circuit Current	10mA min (25mA typ)
FREQUENCY RESPONSE	
Unity Gain, Small Signal	350kHz
Full Power Response	5kHz min (16kHz typ)
Slew Rate Inverting Unity Gain	0.3V/μs min (1.0V/μs typ)
Overload Recovery Inverting Unity Gain	100μs max (16μs typ)
INPUT OFFSET VOLTAGE (Note 3)	3.0mV max (0.4mV typ)
vs. Temperature, T_A = min to max	50μV/°C max
vs. Supply, T_A = min to max	400μV/V max (50μV/V typ)
INPUT BIAS CURRENT	
Either Input (Note 4)	300fA max
INPUT IMPEDANCE	
Differential	$1.6pF \| 10^{13}\Omega$
Common Mode	$0.8pF \| 10^{15}\Omega$
INPUT NOISE	
Voltage, 0.1Hz to 10Hz	4.0μV (p-p)
f = 10Hz	$75nV/\sqrt{Hz}$
f = 100Hz	$55nV/\sqrt{Hz}$
f = 1kHz	$50nV/\sqrt{Hz}$
Current, 0.1 to 10Hz	0.003pA (p-p)
10Hz to 10kHz	0.01pA rms
INPUT VOLTAGE RANGE	
Differential	±20V min
Common Mode, T_A = min to max	±10V min (±12V typ)
Common Mode Rejection, V_{IN} = ±10V	66dB min (94dB typ)
Maximum Safe Input Voltage (Note 5)	$\pm V_S$
POWER SUPPLY	
Rated Performance	±15V typ
Operating	±5V min (±18V max)
Quiescent Current	1.5mA max (0.8mA typ)
TEMPERATURE	
Operating, Rated Performance	0 to +70°C
Storage	-65°C to +150°C
PRICE	
(1-24)	$16.00
(25-99)	$12.50
(100-999)	$ 9.90

For the use of the developed system as a voltage amplifier the magnitude of voltage measured in mechanically stressed bone is on the order of millivolts.[7,13,15] Since the range of the Fourier Analyzer which was used to store and display the data is also millivolts, a gain of 11 was chosen for the voltage amplifier in order to maximize the speed of response (Equation (37)) and yet to easily display the data. Thus, R_3 was chosen to be 10 kiloohms and R_2 was 1 kiloohm.

In order to develop a system which could measure either voltage or current two double pole, double throw switches were used. Both switches were teflon insulated to minimize the leakage in the transduction system. The complete schematic of the developed system is depicted in Figure 10.

II. PREPARATION OF THE BONE SAMPLES

The bone specimens used were machine-formed from embalmed human femur which were obtained from The University of Tennessee School of Dentistry, Department of Dental Anatomy, Memphis, Tennessee. The femur had been stored in a freezer for one year prior to experimentation. Since the identities, causes of death, and ages of the donors were unavailable, a few milled samples (4x and 10x) were subjected to compressive tests in order to insure the normality of the femur used. The tests were performed with an Instron loading device, compressing the bone perpendicular to the bone axis with a loading speed of .02 inches/minute. The ultimate strength of the two samples tested were 75 and 77 pounds. Previously reported literature values for the

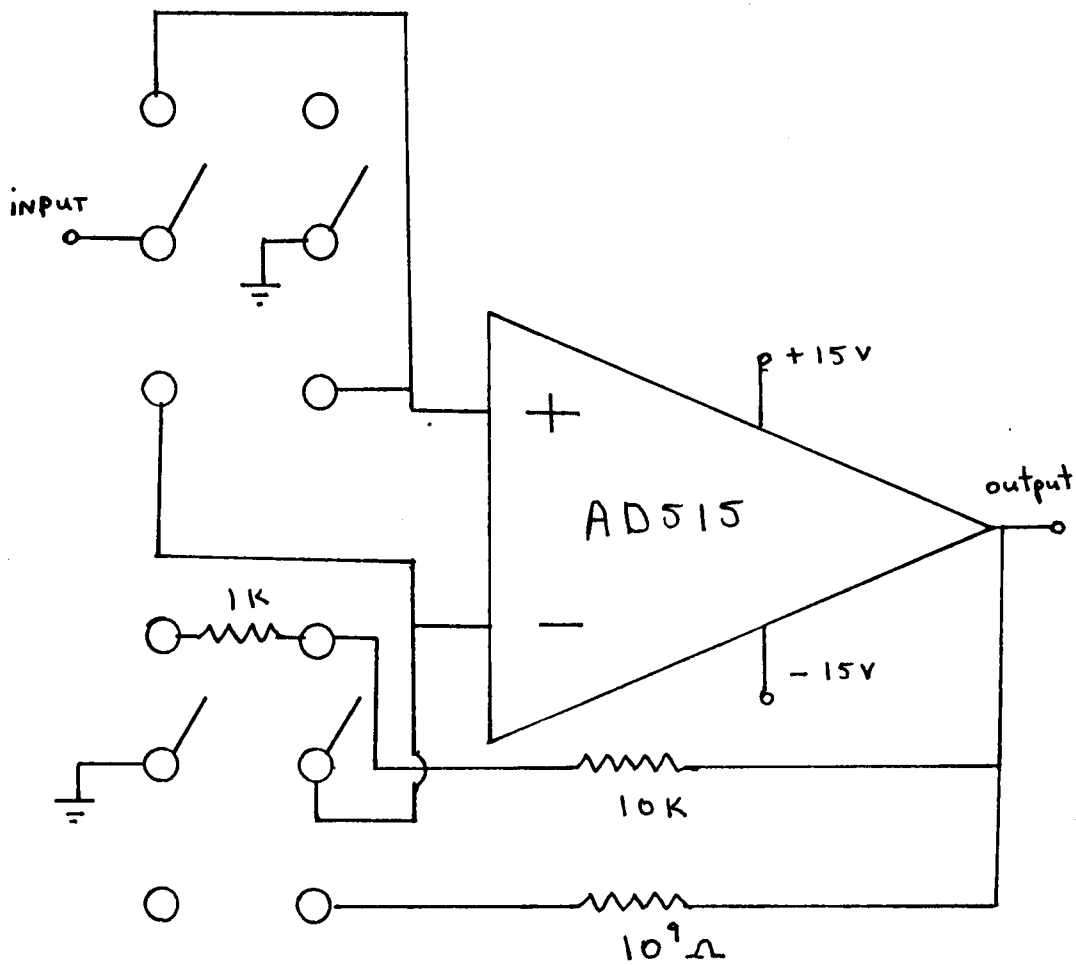

Figure 10. Schematic of the Developed System.

ultimate strength of a $3mm^2$ sample of human femur range from 79.65 to 225.9 pounds.[30] However, it was also pointed out in the literature that slow loading speeds, as were used in this test to prevent damage to the Instron device, would lower the value of the ultimate strength up to 50%. Thus the samples used in this study are well within the range of normal human femur.

Milling Procedures

Whole femurs were sectioned into small rectangular bars, 30 millimeters in length, 3 millimeters in width, and 1 to 2 millimeters in thickness. The sequential process of milling the samples is depicted in Figure 11. Initial lateral sections were cut from the whole femur using a standard bandsaw. Next, two parallel longitudinal cuts were made in each section to obtain a slice of bone which could be held in a milling machine and sectioned with a small radial, circular milling blade. The blade was chosen to have a small radius (1.375 inches) and comparatively large thickness (.045 inches) to prevent its bending during the cutting operation. A 3 millimeter slice was then cut from the top and bottom of each section with the milling machine. Compressed air was used to cool the specimens while cutting in order to avoid exposing the bone samples to excessive heat. The 3 millimeter slices were in turn cut into 1, 1.5, and 2 millimeter sections thus obtaining rectangular bars of human femur. A holding apparatus was constructed so that the bars could be uniformly cut to length. Finally, a hole was drilled in the end of

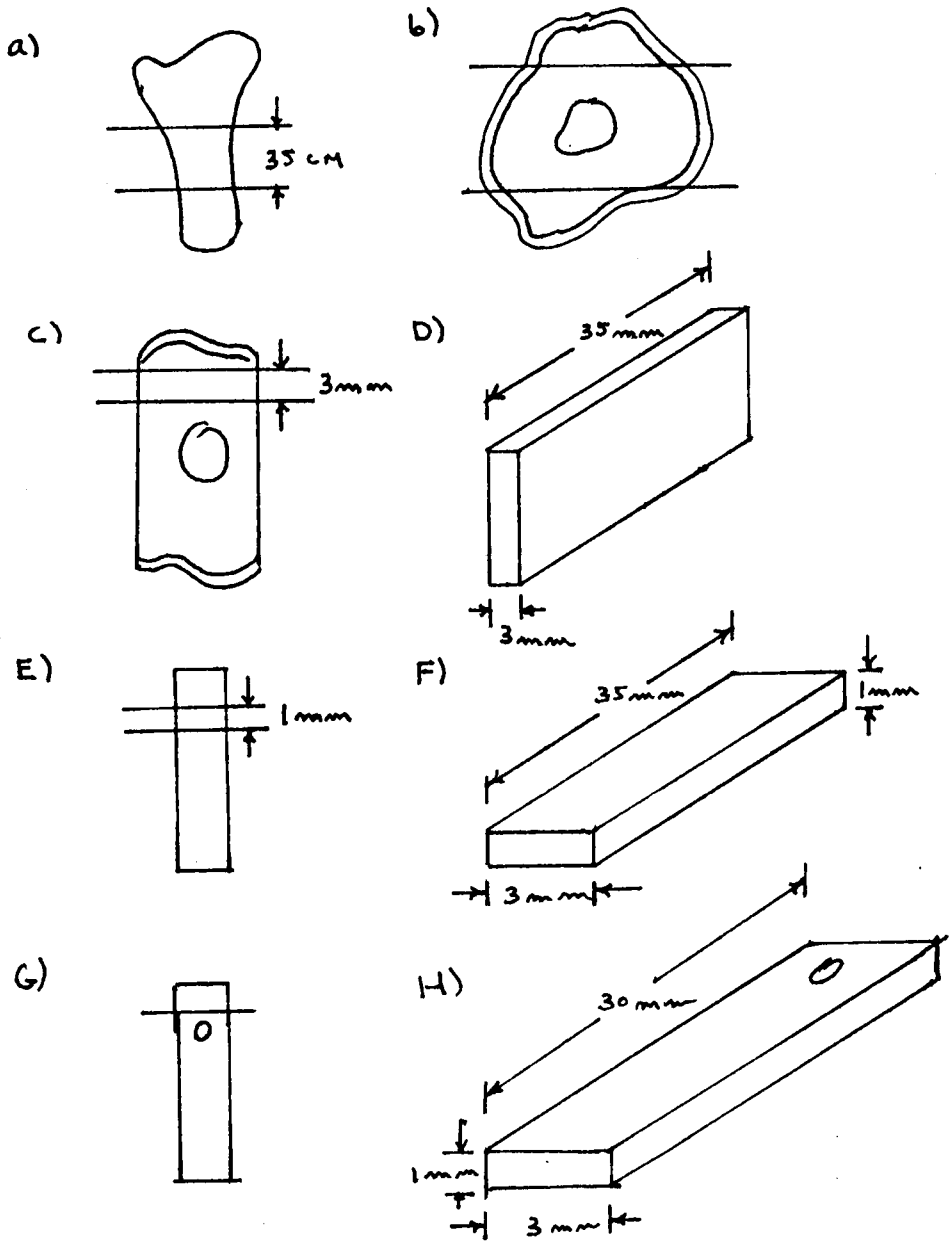

Figure 11. Milling the Samples.

each specimen using a drill press with a number 60 bit. The distance from the base of the Trochanter, the three dimensional location, and the thickness of each specimen used is given in Table 2.

Hydration State of Samples

It is important to define the state of hydration of the bone specimens because it is thought that the piezoelectric response is a function of moisture content as discussed above in Chapter III. There are three techniques which have been described previously in the literature for drying bone samples used in piezoelectric experiments:

1. Oven drying,[10,12]
2. Desiccation,[4,14]
3. Air drying.[6]

In this research, two groups of bone were tested. One group consisted of specimens milled from femurs 1 and 2 and dried in an oven at 80°C for times of from 1 to 3 hours until the weights of the samples reached equilibrium. Since any heat or chemical treatment may alter the ultrastructure of bone,[22] the second group, milled from femur 3, was allowed the air dry from 8 to 12 weeks.

III. EXPERIMENTAL PROTOCOL FOR THE MEASUREMENT OF THE ELECTRIC RESPONSE IN BONE SPECIMENS

There are three types of experiments which have been performed to measure the electric response of stressed bone:

1. Uniaxial compression of milled bone cubes;[4,9,11,12,14,17]
2. Cantilever bending of milled rectangular bars of bone;[1,15,18]
3. Bending of whole bones.[6-8,10,13]

Table 2. Orientation of Milled Bone Samples

Sample #	Location from Base of Greater Trochanter (mm)	Orientation	Thickness (mm)
1x	91	V	1
2x	91	V	1
3x	91	V	2
4x	91	D	1
5x	91	D	1.5
6x	91	D	1
7x	91	D	1
8x	91	D	1
9x	126	V	1
10x	126	V	1
11x	126	V	1
12y	108	L	1
13y	108	L	1
14y	108	L	1
15y	108	L	1
16y	108	L	1
1a	190	D	1.5
2a	190	D	1.5
3a	190	D	1.5
4a	190	D	1.5
5a	190	V	1.5
6a	155	V	2
7a	155	V	2
8a	155	V	2
9a	155	D	1.5
10a	155	D	2

x = femur 1 V = Ventral

y = femur 2 D = Dorsal

a = femur 3 L = Lateral

Since the major focus of this research is the transduction system rather than the specific mode of loading of bone specimens, the cantilever bending experiment was chosen due to the ease of implementation. Three systems for applying loads in cantilever beam experiments have been described previously:

1. Weights hung from the end of the beam;[18,20]
2. Piezoelectric driver in contact with the end of the beam;[1]
3. Pneumatic piston in contact with the end of the beam.[5]

For convenience in this investigation, loads were applied by hanging weights attached by a string to the end of the bone specimens.

Electrodes

In many previous investigations of bone piezoelectricity silver electrodes were used for signal pick up either in the form of silver paint[7,20] or silver epoxy.[9-11,17,25] Based on preliminary experimentation it was discovered that silver epoxy required exposure to high temperatures (150°C) in order to cure properly within a reasonable time period, thus silver paint which cures at room temperature in about 30 minutes was selected to prevent any damage to the bone ultrastructure from excessive heating.

Cochran found that the piezoelectric response of stressed bone in cantilever bending varied with electrode position and determined experimentally the electrode placement for obtaining the largest potential difference.[31] In this research the same electrode placement utilized by Cochran was used to maximize the signal. Thus, with 10 millimeters of the anatomic proximal end of the specimen in a clamp, electrode A

(Figure 12) was painted 2.5 millimeters from the clamp on the concave aspect of the beam and electrode B was painted 2.5 millimeters from the load on the convex aspect of the beam. The strips of paint were 1 to 2 millimeters in width and were applied across the entire width of the bone specimen. A plexiglass jig was fashioned to insure reproducibility of the electrode placement. A gold wire electrode manufactured by Leeds and Northrup Co., Philadelphia, Pennsylvania, was then glued to the silver strip with five minute epoxy in order to interface between the silver electrode and the amplifier. Good electrical contact was maintained by painting a thin strip of silver from the unglued portion of the gold electrode to the silver strip on the specimen. (See Figure 12.)

Cantilever Beam Jig

In order to prohibit any electrical leakage of the signal, the clamp holding the bone specimen was made from plexiglass, a good insulator ($\rho = 1 \times 10^{+15}$ ohms). A slot, 10 millimeters in length was milled in the clamp to insure that all specimens were positioned uniformly. The clamp was then mounted directly on the aluminum box housing the amplifier as shown in Figure 13, thus minimizing any stray capacitance in the connecting leads which might cause instabilities in the amplifier as discussed above.

Preliminary Considerations

Once the bone specimen had been positioned in the clamp, electrode A was soldered to a pin which in turn was fitted into the

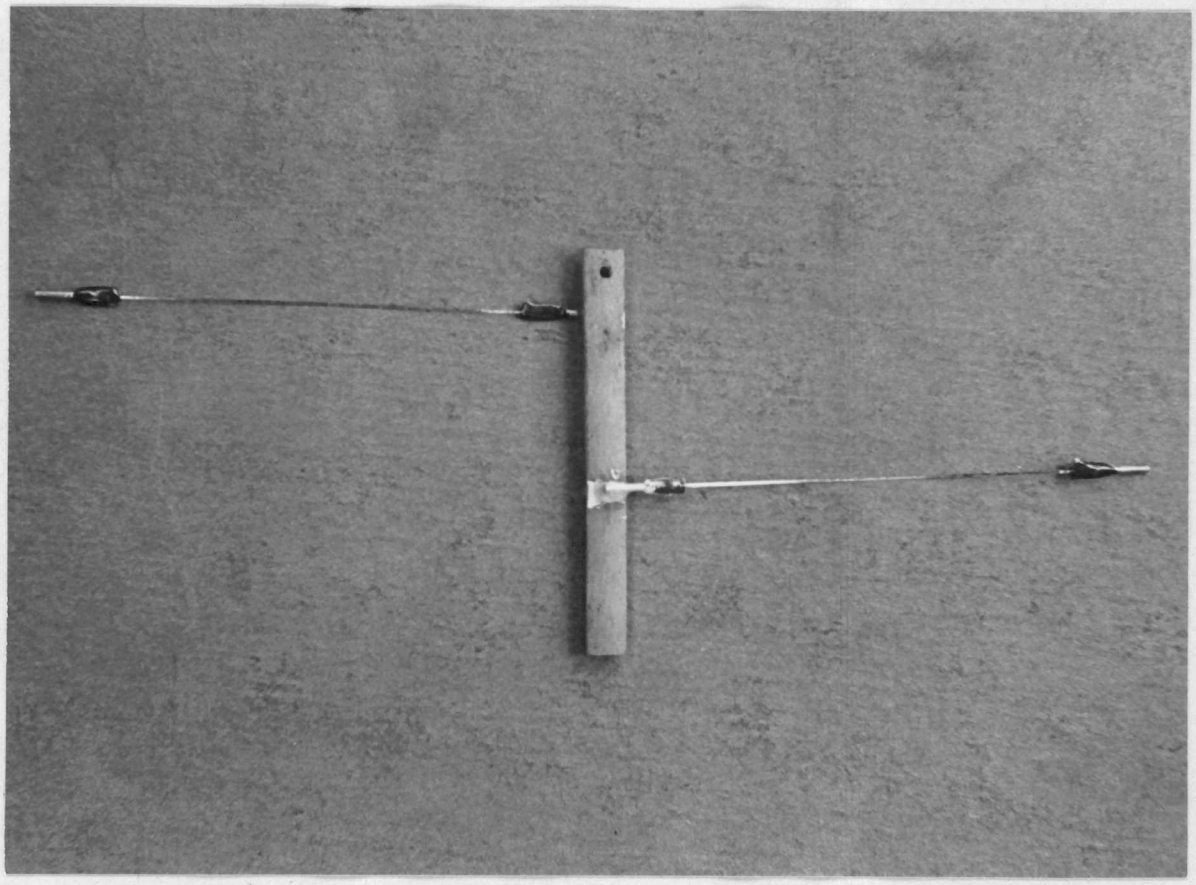

Figure 12. Photograph of the Electrodes on the Specimen.

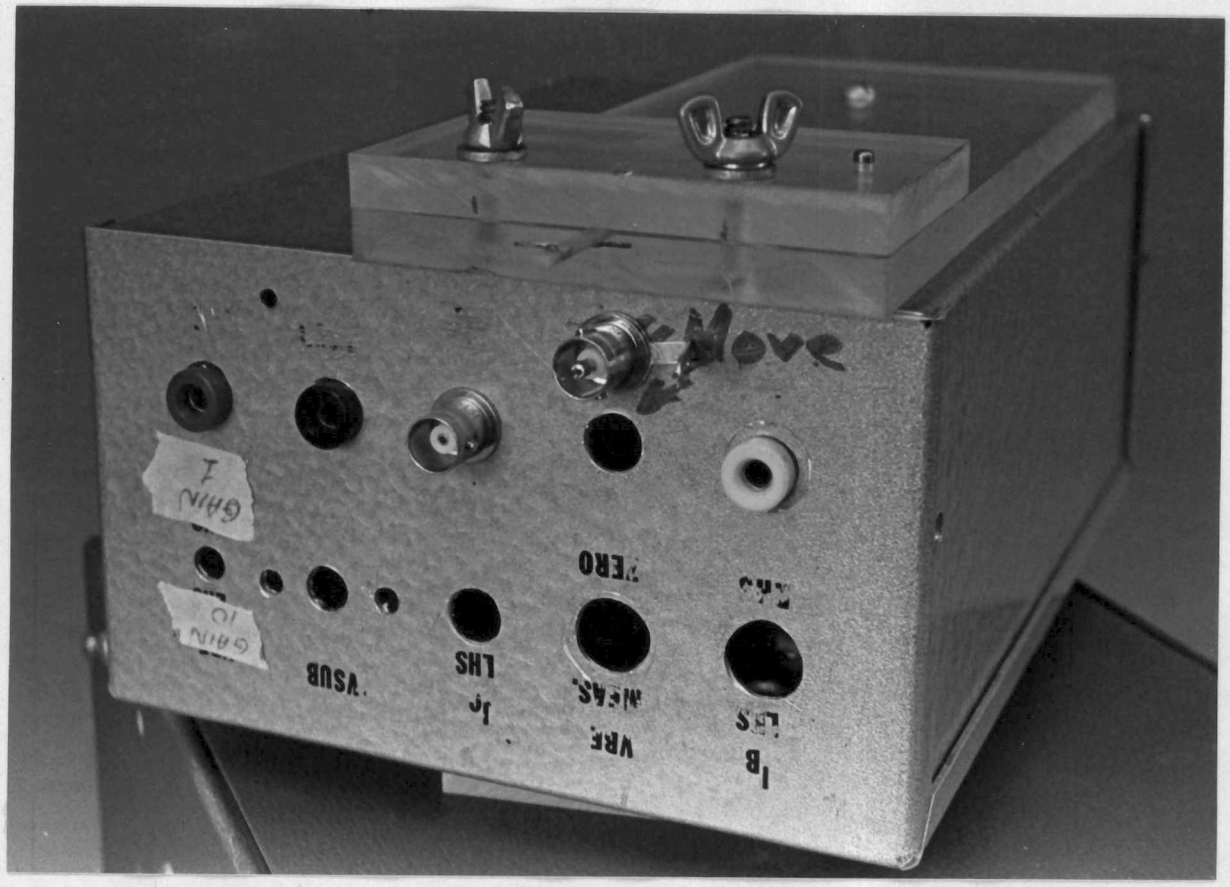

Figure 13. Photograph of the Clamp Mounted on the Amplifier.

BNC input of the amplifier. (See Figure 13.) A string with a knot on one end was then threaded through the hole in the bone specimen in order to attach weights to the sample. Finally, the cantilever beam jig, bone specimen, and amplifier were enclosed in a grounded steel box to shield the experiment from any electrical or electromagnetic interference. One hole had been drilled in the steel box directly beneath the bone specimen so that the sample could be loaded externally, and three holes had been drilled in the front panel for the power supply and output leads. (See Figure 14.)

Experimental Procedure

Weights ranging from 1/16 to 2 ounces were used to load the specimen yielding steady state end deflections of 0.5 to 1 millimeters. Loading was accomplished by tying the weight to the string which was attached to the end of the bone specimen. Each weight was then dropped from a position of about 1 centimeter above the "loaded position," thus simulating an instantaneous applied load. The electrical output was recorded on a Hewlett-Packard Model 5420 A Digital Signal Analyzer with a model 9872A Digital plotter for data display. Three types of loading experiments were performed: (1) loading—unloading; (2) progressive loading; and (3) fatigue loading.

Loading—unloading. Since the basic piezoelectric waveform was being investigated, a moderate size load (1/2 ounce) was applied to the specimen and then manually unloaded. Both current and voltage waveforms were obtained for specimens of different thicknesses.

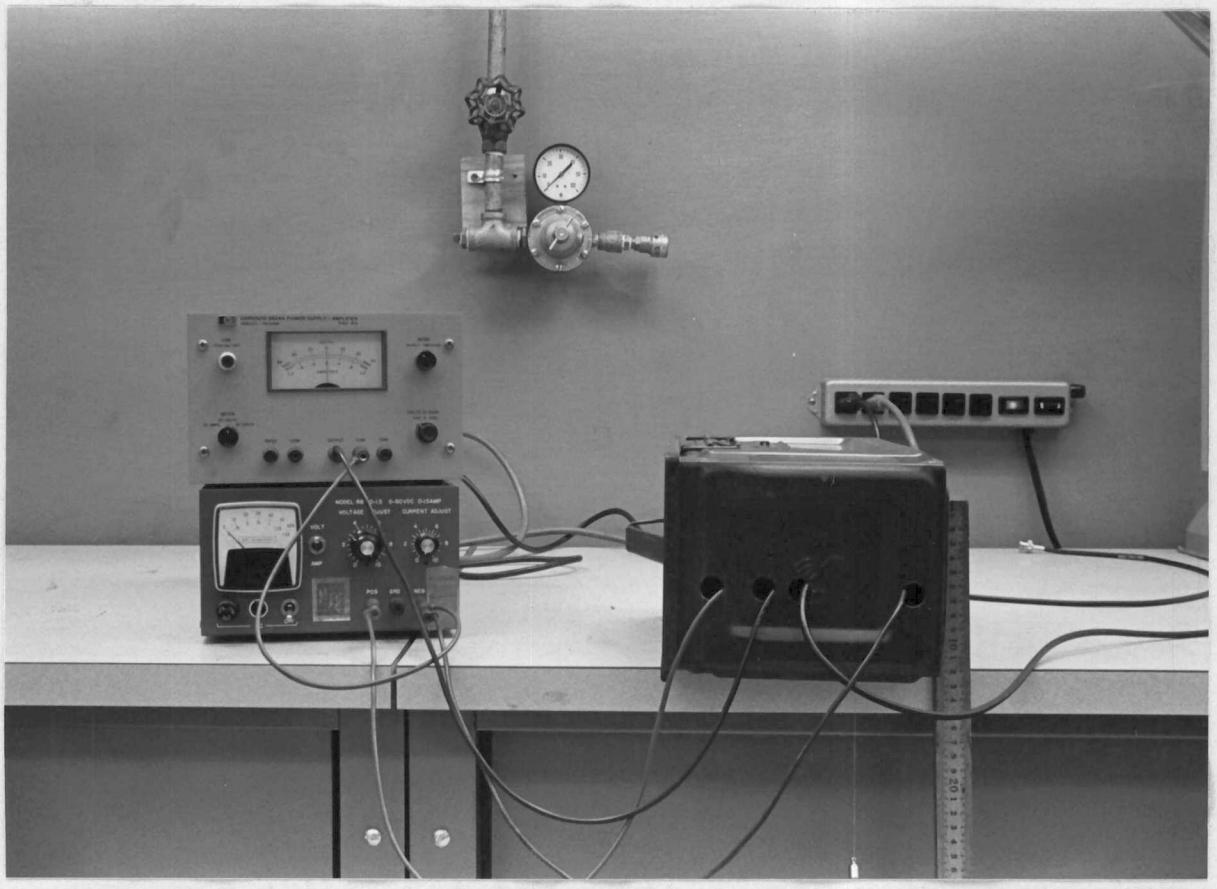

Figure 14. Photograph of Experimental Setup.

Progressive loading. To insure that the results of these experiments were not artifact, progressively larger loads were applied to the bone samples (1/16 to 2 ounces). The magnitude of the voltage and current waveforms were then examined to assure that the electrical response increased with increasing stress as predicted by theory and previous experiment.

Fatigue loading. A moderate size load (1/2 ounce) was repeatedly applied to a given bone sample to determine if any deviation in the piezoelectric response resulted from subsequent experimentation. Both current and voltage waveforms were examined.

CHAPTER VI

RESULTS

The results of the theoretical analysis established in Chapter IV as well as the results of the experimental analysis as outlined in Chapter V are presented in this chapter.

I. THEORETICAL RESULTS

Rise Time

The rise time of a transduction system is given by Equation (37), page 39. By examining the transfer function of the voltage amplifier Equation (13), page 27, it can be seen that the -3dB frequency is a function of the source resistance R_g, whereas the -3dB frequency of the current amplifier, calculated from Equation (15), page 28, is independent of R_g. Thus, in this analysis, the rise time of the voltage amplifier was calculated as a function of R_g using the specifications of the AD515 amplifier given in Table 1, page 43, and with R_2 equal to 1 kiloohm and R_3 equal to 10 kiloohms. Since the capacitance of dry bone has not been documented in the literature, a conservative value of 2 picofarads was chosen for C_g. Transforming the voltage transfer function to the frequency domain, Equation (40) is obtained assuming $R_B >> R_g$ (see Table 1, page 43), thus:

$$\frac{V_o}{I_1} = \frac{R_g\left(\frac{R_2 + R_3}{R_2}\right)}{1 - f^2 \Big/ \frac{A_o \omega_o}{R_g}\left(\frac{R_2}{R_2 + R_3}\right)}$$

$$+ j\left[f \Big/ A_o \omega_o \left(\frac{R_2}{R_2 + R_3}\right) + f \Big/ \frac{1}{2\pi R_g C_g}\right] \qquad (40)$$

Substituting the values specified above, Equation (40) becomes:

$$\frac{V_o}{I_1} = \frac{R_g\ (11)}{1 - \frac{f^2}{\frac{1}{R_g}\left(1.59 \times 10^{16}\right)}}$$

$$+ j\left[\frac{f}{32 \times 10^3} + \frac{f}{\frac{1}{R_g}\left(7.96 \times 10^{10}\right)}\right] \qquad (41)$$

From this equation the -3dB frequency was determined for values of R_g ranging from 10^3 to 10^9 ohms, and Equation (37) was used to calculate the corresponding rise times. A plot of rise time versus R_g for the voltage amplifier is given in Figure 15.

Thus, from this plot it can be seen that the speed of response of the voltage amplifier is very much diminished as source resistance increases even though a very small value of source capacitance is assumed. From Equation (40) it can be shown that for larger values of source capacitance, as is the case in moist bone, the speed of response of the voltage amplifier is diminished to an even greater extent.

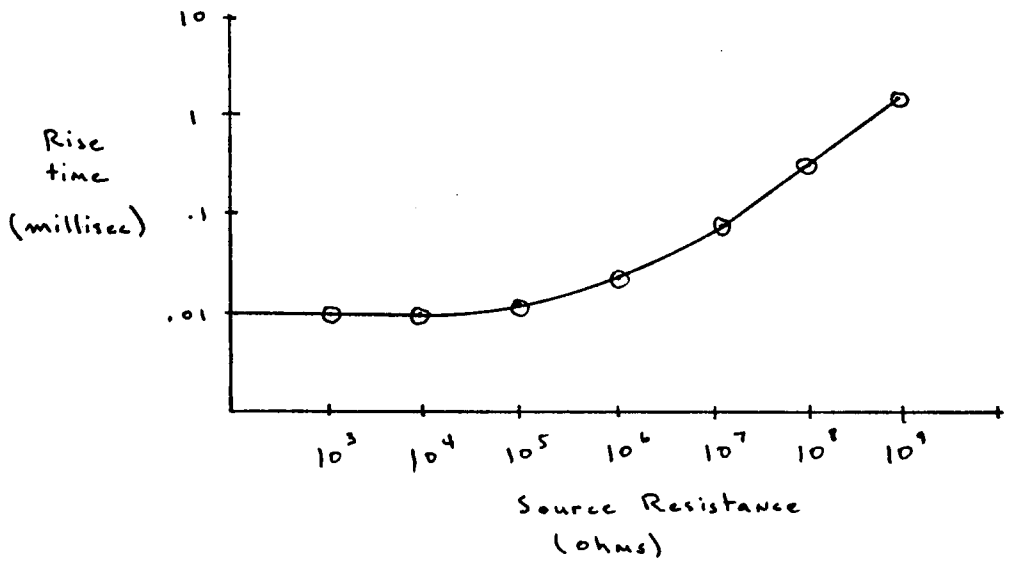

Figure 15. Plot of Rise Time Versus Source Resistance for a Voltage Amplifier with 2 Picofarads of Source Capacitance.

For the current amplifier it is instructive to examine for what case R_g is important in determining the speed of response. Thus solving the Equation (14), page 28, for $\frac{V_o}{I_1}$ the unsimplified form of Equation (15), page 28, is obtained:

$$\frac{V_o}{I_1} = \frac{s\left[\frac{R_g R_o}{\omega_o\left(A_o R_g + R_f\right)}\right] - \frac{R_g A_o R_f}{A_o R_g + R_f}}{s^2\left[\frac{R_f R_g C_g}{\left(A_o R_g + R_f\right)\omega_o}\right] + s\left[\frac{R_f R_g C_g}{A_o R_g + R_f} + \frac{R_g}{\left(A_o R_g + R_f\right)\omega_o} + \frac{R_f}{\left(A_o R_g + R_f\right)\omega_o} + \frac{R_f R_g}{\left(A_o R_g + R_f\right) R_1 \omega_o}\right] + 1} \qquad (42)$$

Therefore, for $R_g A_o >> R_f$ Equation (42) reduces to the form of Equation (15) which is independent of R_g. This assumption is valid for measurements of the electrical response of bone because, as discussed above in Chapter III, literature values of R_g range from 10^9 to 10^{12} ohms. Thus transforming Equation (15) to the frequency domain in order to examine the speed of response of the current amplifier and assuming $R_1 >> R_f$ (see Table 1, page 43), the result is:

$$\frac{V_o}{I_1} = \frac{\left[j f \Big/ \frac{A_o \omega_o}{R_o} - R_f \right]}{1 - f^2 \Big/ \frac{A_o \omega_o}{R_f C_g} + j \left[f \Big/ \frac{A_o}{2\pi R_g C_g} + f \Big/ A_o \omega_o \right] + 1} \qquad (43)$$

For R_f equal to 10^9 ohms and assuming C_g is 2 picofarads as before, the rise time of the AD515 op amp used as a current amplifier was found to be .0171 milliseconds. Thus, the current amplifier has a much faster response than the voltage amplifier when the source resistance is 10^9 ohms.

Stability

The stability of the AD515 op amp in the current, charge, and voltage amplification configurations was examined as described above in Chapter IV. In this analysis the value of the source resistance was varied from 10^9 to 10^6 ohms and the value of the source capacitance was varied from 10^{-12} to 10^{-5} farads in the characteristic equation to simulate bone going from a dry state to an in vivo wet state.

Using the computer to solve for the roots of the characteristic equation, the voltage amplifier was found to be stable under all conditions with gains from 11 to 1100. The charge amplifier was also stable under all conditions as R_f varied from 10^{11} to 10^7 ohms and C_f from 10^{-9} to 10^{-6} farads. The current amplifier, however, had a tendency towards instability for source capacitances between 10^{-12} and 10^{-9} farads with R_f equal to 10^9 ohms. This result is expected due to the fact that in a current amplifier, the source impedence

is a part of the feedback network and thus interacts with the pole created by the amplifier. Instabilities of this type can be corrected, as stated in the manufacturer's notes and as can be seen from Equation (18), page 30, by placing a small shunt capacitor around the feedback resistor. However, as can also be seen by examining Equation (18), when the shunt capacitor is added, the bandwidth, and therefore the speed of response is limited.

Noise Analysis

Equations (34), page 36, and (36), page 37, were used to determine the noise level of the voltage and current transduction systems respectively. Since the impedence of bone varies with moisture content as discussed above in Chapter IV, two extreme cases were investigated in this analysis:

1. All terms containing R_g in the noise equation are insignificant;
2. All terms containing R_g are significant (with R_g assumed equal to 10^9 ohms).

Voltage amplifier. With R_2 equal to 1 kiloohm and R_3 equal to 10 kiloohms, the equivalent input noise $\overline{E_{ni}^2}$ becomes 2.66×10^{-6} volts^2. Thus, for the worst case, the order of magnitude of the smallest detectable signal is the square root of 2.66×10^{-6} volts^2 or approximately one millivolt, which should be sufficient to measure voltage obtained from mechanically stressed bone.

Current amplifier. The equivalent input noise voltage $\overline{E_{ni}^2}$ of the current amplifier was calculated using Equation (36). Since the equivalent input noise current $\overline{I_{ni}^2}$ is given by:[28]

$$\overline{I_{ni}^2} = \frac{4KT}{R} \tag{44}$$

and the equivalent input noise voltage $\overline{E_{ni}^2}$ is given by:[28]

$$\overline{E_{ni}^2} = 4KTR \tag{45}$$

Equations (44) and (45) can be solved simultaneously to obtain $\overline{I_{ni}^2}$ for the current amplifier. Therefore, with R_f equal to 10^9 ohms, neglecting all R_g terms, $\overline{I_{ni}^2}$ was found to be 1.8×10^{-21} amps^2. With R_g equal to 10^9 ohms, $\overline{I_{ni}^2}$ is equal to 1.325×10^{-25} amps^2. Thus, for the worst case (R_g terms are negligible in Equation (36)) the minimum amplifiable signal for the current amplifier would be on the order of 10^{-11} amps. Although there is no data on bone current generation, this high sensitivity should be adequate to measure current from mechanically stressed bone.

II. EXPERIMENTAL RESULTS

The experimental protocol is detailed in Chapter V. Three experiments were performed: (1) progressive loading; (b) loading and unloading; and (3) fatigue loading. Since the size of the specimens, electrode placement, and experimental protocol correspond to that used by Cochran et al.,[15] their previously reported results were used to demonstrate the ability of the systems and methods used in

this work to produce electrical signals with generally known salient characteristics.

Progressive Loading

Sample plots of the data obtained in the progressive loading experiments are given in Figures 16 and 17. Additional data from these experiments is displayed in Figures 21-29 in Appendix A. In each plot the vertical axis is in millivolts and the horizontal plot is in seconds. A time delay was used in plotting the data to obtain the position of the neutral baseline before loading. The magnitude of the electric response was obtained by dividing the peak magnitude of the waveform in each plot by the D.C. gain of the respective amplifier used to make the measurement. The D.C. gain of the voltage amplifier as calculated from Equation (38), page 40, is 11 volts/volt and the D.C. gain of the current amplifier as calculated from Equation (39), page 41, is 1 volt/nanoamp. Thus in the experiments described here, the magnitude of voltage measured in pieces of mechanically stressed human femur ranged from 2 millivolts to 37 millivolts and the magnitude of current varied from 1.5 pico amps to 100 pico amps. Cochran et al. reported values of voltage from 0.5 millivolts to 20 millivolts with an average of about 3 millivolts with the use of larger loads (200 to 500 grams) than those used in the present work (1.7 grams to 108.8 grams). As can be seen from Figures 21-29 in Appendix A, the peak magnitude of both the voltage and current increased with increasing load as predicted from classical piezoelectric theory giving evidence that the signals

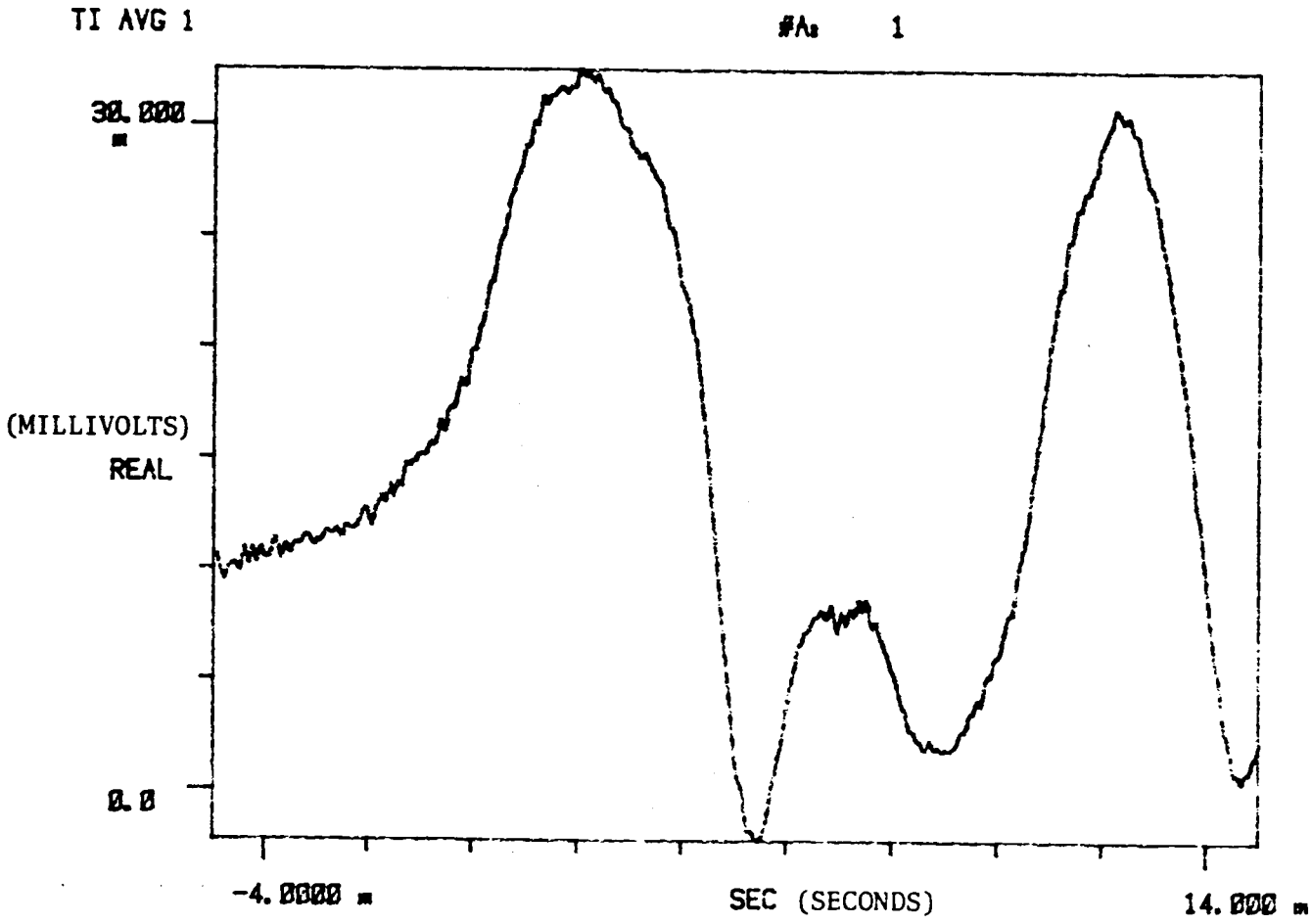

Figure 16. Sample Current Waveform Obtained in the Progressive Loading Experiment.

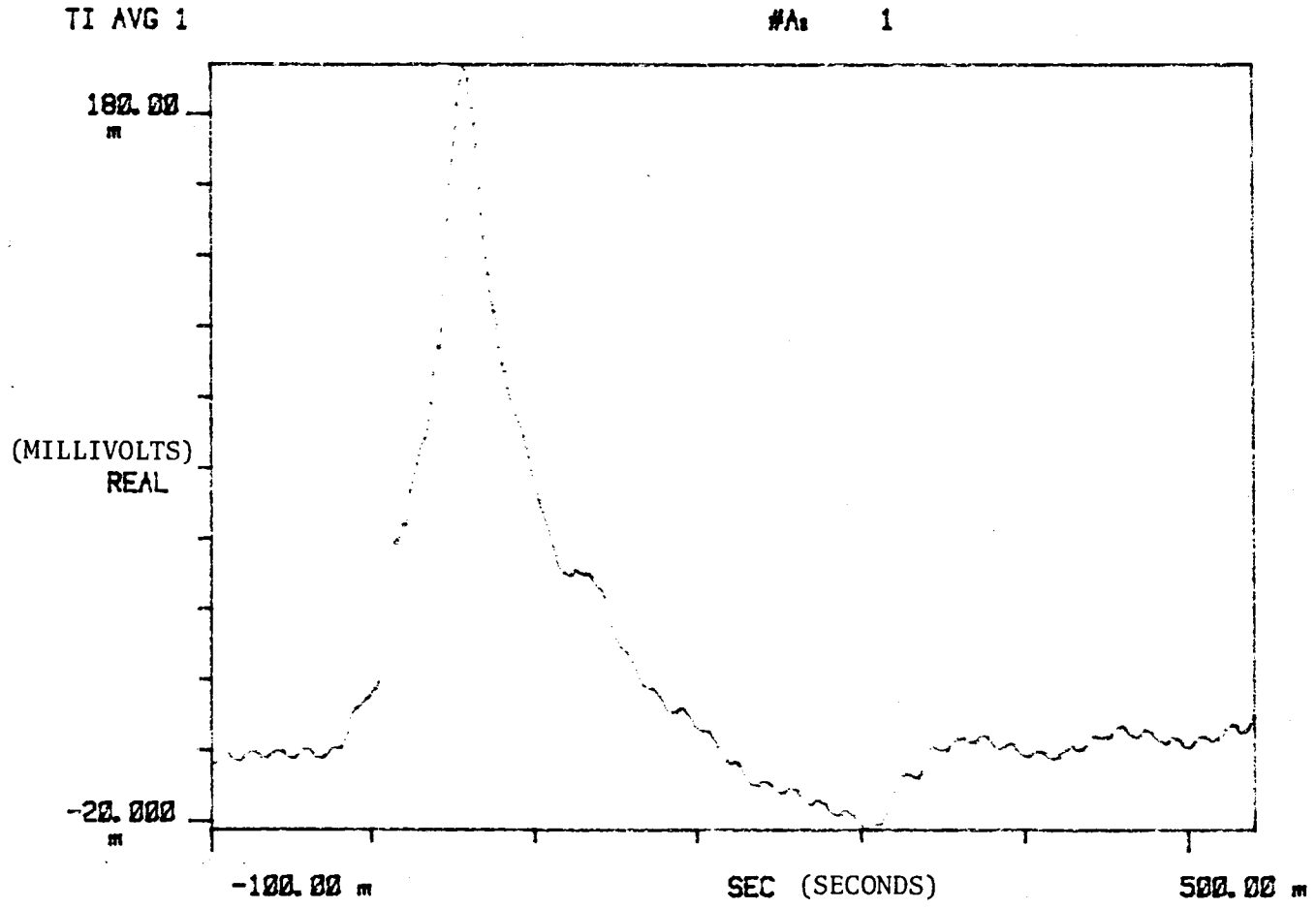

Figure 17. Sample Voltage Waveform Obtained in the Progressive Loading Experiment.

are not artifact. No attempt was made to quantitatively correlate the magnitude of the load with the electric response due to the limitations inherent in the loading technique used.

Voltage and Current Waveform

The voltage waveforms obtained in this research (see Figure 18) are identical to those reported by Cochran[15] and others.[6-8,13] Upon loading, for all measurements made, the convex portion of the beam became positive while the concave portion of the beam always became negative. The signal decayed to the baseline within 0.5 to 2 seconds after the load was applied and a wave of similar shape but opposite polarity and from 10-50% less amplitude occurred upon removal of the load.

The current waveforms obtained in these experiments (a typical signal plot is presented in Figure 19) were substantially different from those for voltage measurement. As can be seen from Figure 19, the wave has the appearance of a damped sinusoidal response. Upon loading, both positive and negative currents were detected, but the positive currents dominated the response. Similarly, negative currents dominated the electric response when the load was removed. Thus, it can be concluded that the second pulse obtained in the voltage waveform is not artifact, since reverse currents are present and the latter are dominant upon removal of the load. The current waveform always returned to the neutral baseline within a maximum of 0.5 seconds, thus, within the resolution of the current amplifier used for all current measurements (1×10^{-13} amps), no low level D.C. currents were present.

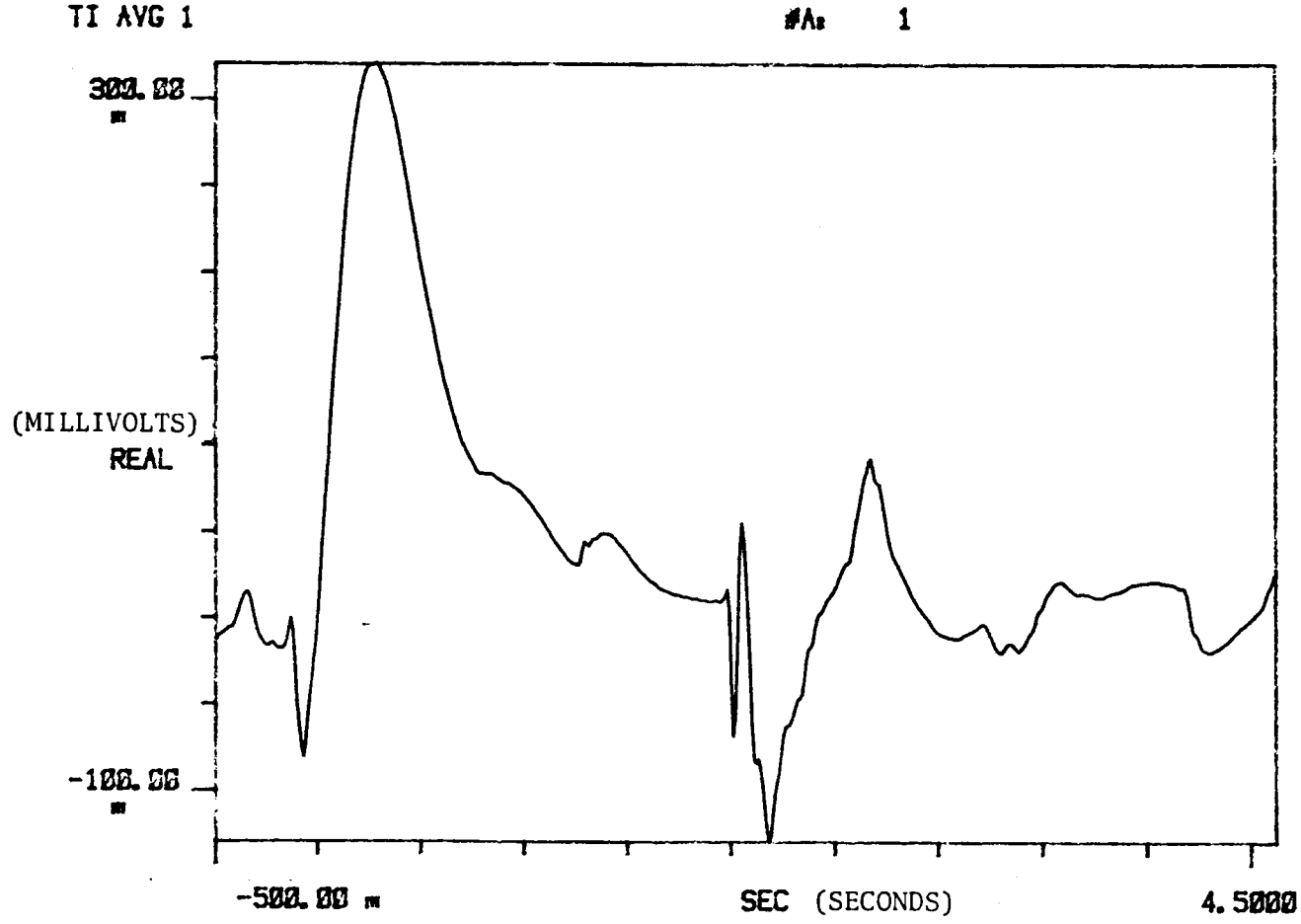

Figure 18. Typical Voltage Waveform Obtained from Sample 3x Using a 1/2 Ounce Load.

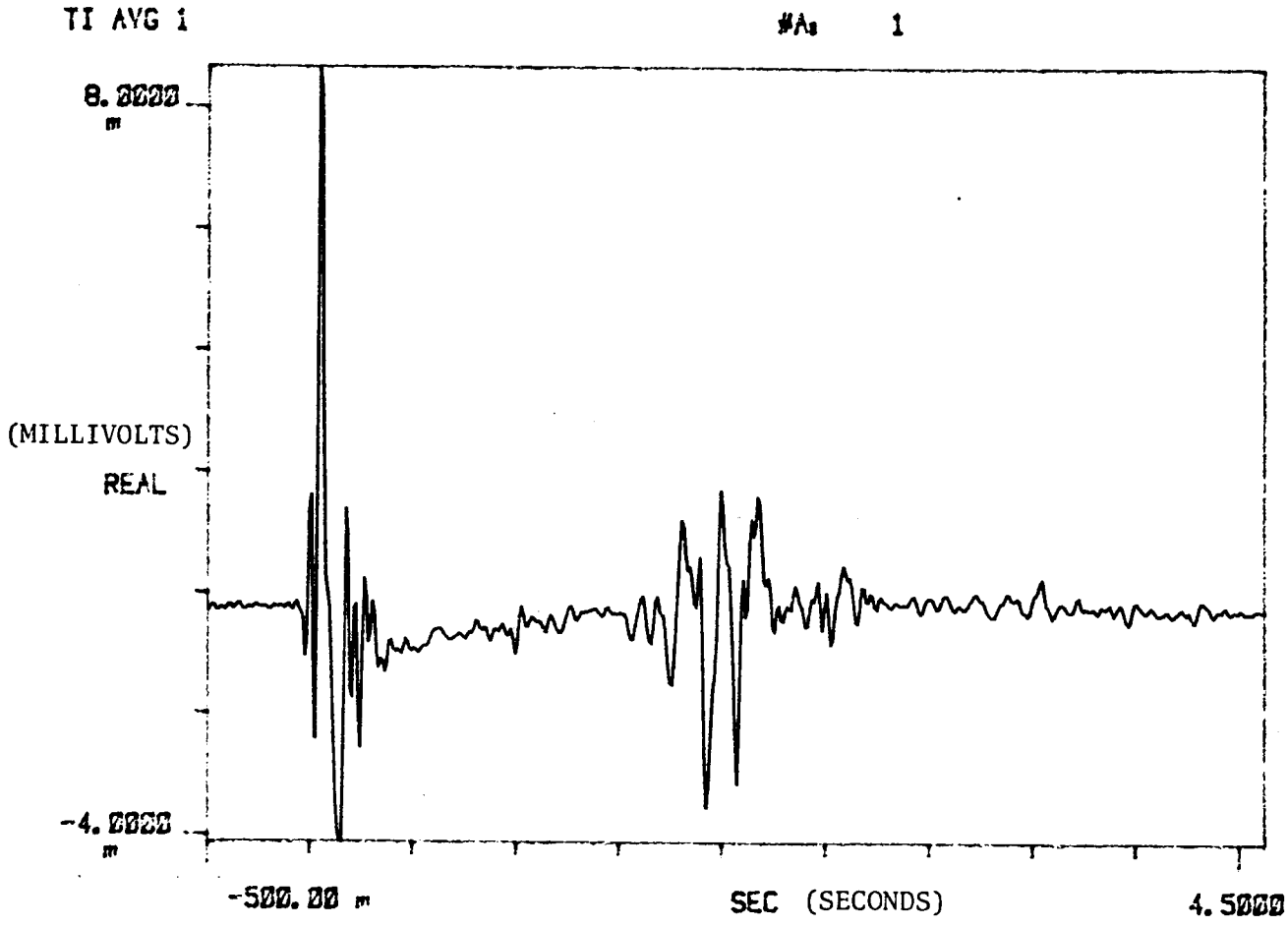

Figure 19. Typical Current Waveform Obtained from Sample 3x Using a 1/2 Ounce Load.

Fatigue Loading Experiments

A sample plot from the fatigue loading experiments is shown in Figure 20 where the current waveform is depicted on top and the voltage waveform on bottom. Additional results of the fatigue loading experiments are displayed in Figures 30-38 in Appendix B. From this data it can be seen that little detectable change occurred in the overall shape of the waveform of either the current or voltage signal. However, substantial changes were recorded in the magnitude of the electric signal, especially the voltage, upon repeated loading of a single bone specimen. Cochran noted only slight variations in the voltage response in fatigue experiments with a given bone specimen up to the yield point,[15] thus indicating that the loading technique used in this research needs to be refined before further quantitative studies are conducted.

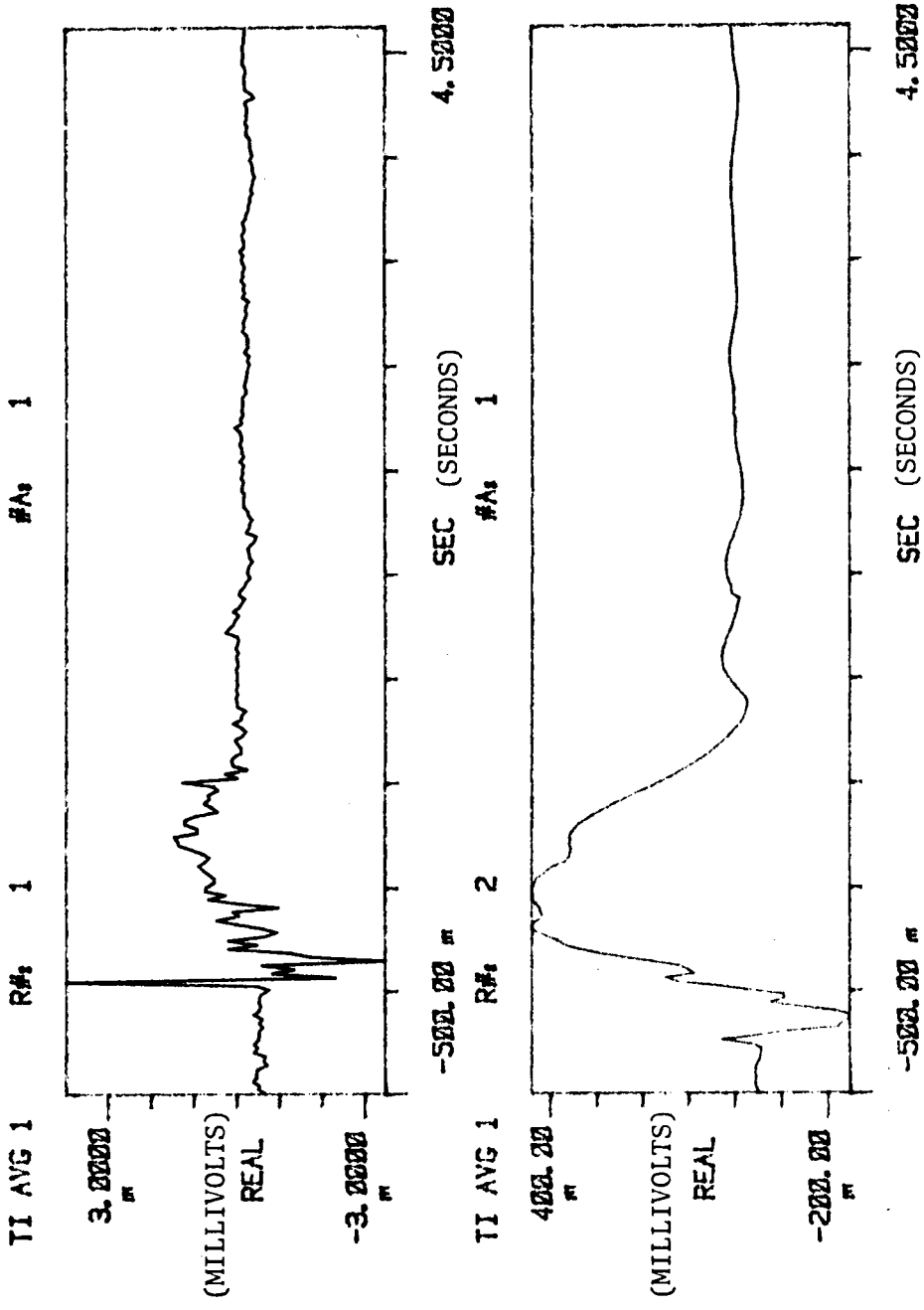

Figure 20. Sample Data Obtained from the Fatigue Loading Experiment.

CHAPTER VII

DISCUSSION

In this chapter conclusions from examining the current waveform are drawn, and a comparison of the voltage and current waveforms is made. Also limitations of each transduction system in particular the rise time and signal to noise ratio are discussed.

I. RISE TIME

In comparing the voltage and current waveform obtained from the same specimen (Figures 18 and 19, pages 68 and 69), it appears that the voltage amplifier essentially integrates the current. This result follows from the theory, for as discussed above, the rise time of the voltage amplifier is a strong function of the source resistance (see Figure 15, page 59), whereas the current amplifier is essentially independent of the source resistance. Thus, for the case of measuring piezoelectricity in a high impedence bone sample, the speed of response of the voltage amplifier is not sufficiently fast to follow the electric response of the mechanically stressed bone, whereas the current amplifier gives an unintegrated reflection of the dynamic stress-electric response relationship. Extreme caution must therefore be used in designing instrumentation to measure bone piezoelectricity, especially in hydrated samples where the increased capacitance limits the speed of response of the voltage amplifier to an even greater extent. The observation made by Cochran,[15] that the voltage signal increased as water evaporated

from the moistened bone samples, verifies this hypothesis for as the water evaporates, the capacitance decreases and thus the attenuation by the voltage amplifier is reduced. The difference in capacitance in the samples used by Cochran and those used in this research may also account for at least part of the difference in the magnitude of the voltage response obtained in the two studies. Furthermore the variation in the waveform magnitude with moisture content discussed in Chapter III may be simply due to differences in the effective time constants of the voltage transduction systems for varying source impedence.

II. RELATIONSHIP BETWEEN ELECTRICAL RESPONSE AND SAMPLE PREPARATION PROCEDURES

In this research it was consistently observed that the magnitude of current generated for constant loads varied greatly depending upon how a specimen was prepared. As can be seen from comparing Figure 19, page 69, with Figure 24 in Appendix A, the magnitude of current generated by a 1/2 ounce load in an oven dried sample (3x) was substantially smaller than that obtained from an air dried sample (10a). However, the magnitude of voltage obtained from sample 3x (Figure 18, page 68) using a 1/2 ounce load and that obtained from the air dried sample 7a (Figure 29 in Appendix A) was identical. As discussed above in Chapter II, previous investigators[8] reported little or no change in the voltage response in stressed bone samples subjected to a variety of preparation techniques. This result is confirmed for the voltage measurements in this research, but due to the significant

change in the magnitude of current obtained from bone samples which were subjected to different treatments prior to experimentation, it must be concluded that sample preparation may be more important in a complete characterization of bone piezoelectric effects than previously thought.

III. SIGNAL TO NOISE RATIO

Using the results of the noise analysis for current and voltage amplifiers, and obtaining an average magnitude for both the current and voltage responses from the experimental data, the signal to noise ratio was calculated for each transduction system assuming R_g equal to 10^9 ohms. For the voltage amplifier, the average signal was approximately 15 millivolts, thus the signal to noise ratio was calculated to be approximately 20 dB. With an average signal of 10 picoamps, the signal to noise ratio for the current amplifier was calculated to be 29 dB. Thus in these experiments, the current amplifier had the best signal to noise ratio. However as can be inferred from the results of the noise analysis as presented in Chapter VI, if the source impedence was smaller, the voltage amplifier would probably have the better signal to noise ratio.

CHAPTER VIII

CONCLUSIONS

In view of the theoretical and experimental results presented in Chapter VI, and the discussion presented in Chapter VII, the principal conclusions established from this research are listed below along with recommendations for further study.

I. INSTRUMENTATION

1. High source impedence values severely restrict the speed of response of the voltage amplifier whereas the speed of response of the current amplifier is essentially independent of the source resistance if $R_g A_o >> R_f$.

2. Since the source impedence of the current amplifier is a part of the feedback loop, the current amplifier had a tendency towards instability for values of source capacitance from 10^{-12} farads to 10^{-9} farads whereas the voltage amplifier was found to be stable under a large variety of source impedences.

3. In this research, the current amplifier had a better signal to noise ratio than the voltage amplifier (29 dB as opposed to 20 dB).

II. EXPERIMENTAL RESULTS

1. The voltage waveform and magnitude obtained from mechanically stressed bone in this research correlated well with those reported previously for similar experimental conditions.

2. The current waveform obtained from mechanically stressed bone was substantially different from the voltage waveform, most probably due to the speed of response of the relative transduction systems.

3. The magnitude of current obtained in this research from mechanically stressed bone varied from 2 picoamps to 100 picoamps and the magnitude of the voltage varied from 2 millivolts to 37 millivolts.

4. The magnitude of the current and voltage response increased with increasing load as predicted from piezoelectric theory, thus giving evidence that the results obtained were not artifactual.

5. Negative currents were present upon removal of the load from the bone specimen, thus indicating that the "second pulse" obtained in the typical voltage waveform is not artifact.

6. Within the resolution of the current amplifier used in this research (1×10^{-13} amps), no low level D.C. currents were detected upon sustained loading.

7. Bone specimens which had been air dried, as opposed to oven dried generated much larger currents upon loading, while the magnitudes of voltage generated were essentially the same.

8. In view of the differences in voltage and current measurements in mechanically stressed bone, both waveforms should be examined in future bone piezoelectricity experiments with the limitations of each transduction system taken into account in order to obtain a more complete understanding of the piezoelectric phenomena.

III. NEED FOR FURTHER RESEARCH

1. A much more sophisticated loading technique than was used in this research should be developed in order to accurately define the dynamic stress-electric response relationship.

2. Current amplification techniques need to be extended to moist bone experiments in order to obtain a more complete understanding of bone piezoelectricity *in vivo*.

3. With more precise loading techniques, the waveform should be examined with faster current amplifiers to insure that the speed of response of the amplifier is not limiting the response.

LIST OF REFERENCES

LIST OF REFERENCES

1. C. A. Bassett, "Electrical Effects in Bone," Scientific American, 213, pp. 18-25, 1955.

2. Z. B. Friedenberg et al., "Healing of Nonunion of the Medial Malleolus by Means of Direct Current: A Case Report," The Journal of Trauma, II, pp. 883-885, 1971.

3. I. Yasuda, Journal of Japanese Orthopaedic Surgery Society, 28, N. 2, 3, 1954, (Referenced in E. Fukada and I. Yasuda, 1957).

4. E. Fukada and I. Yasuda, "On the Piezoelectrictric Effect of Bone," Journal of the Physical Society of Japan, 12, pp. 11-58-1162, 1957.

5. W. S. Williams, "Sources of Piezoelectricity in Tendon and Bone," C R C Critical Review in Bioengineering, 2, pp. 95-118, 1974.

6. C. A. Bassett and R. O. Becker, "Generation of Electrical Potentials by Bone in Response to Mechanical Stress," Science, 137, pp. 1063-1064, 1962.

7. M. H. Shamos, L. S. Lavine, and M. I. Shamos, "Piezoelectric Effect in Bone," Nature, 197, p. 81, 1963.

8. M. E. Steinberg et al., "Electrical Potentials in Stressed Bone," Clinical Orthopaedics and Related Research, 61, pp. 294-299, 1968.

9. A. J. Bur, "Measurements of the Dynamic Piezoelectric Properties of Bone as a Function of Temperature and Humidity," Journal of Biomechanics, 9, pp. 495-507, 1976.

10. J. H. McElhaney, "The Charge Distribution on the Human Femur Due to Load," The Journal of Bone and Joint Surgery, 49-A, pp. 1561-1571, 1967.

11. G. B. Reinish and A. S. Nowick, "Piezoelectric Properties of Bone as Functions of Moisture Content," Nature, 253, pp. 626-627, 1975.

12. A. A. Marino and R. O. Becker, "Piezoelectricity in Hydrated Frozen Bone and Tendon," Nature, 253, pp. 627-628, 1975.

13. P. G. Harms, J. R. Neville, and R. L. Peebles, "Electromechanical Properties of Fresh Whole Bone," SAM-TR-70-44, U S A F School of Aerospace Medicine, Texas, 1970.

14. J. C. Anderson and C. Eriksson, "Piezoelectric Properties of Dry and Wet Bone," Nature, 227, pp. 491-492, 1971.

15. G. V. B. Cochran, R. J. Pawluk, and C. A. L. Bassett, "Electromechanical Characteristics of Bone under Physiologic Moisture Conditions," Clinical Orthopaedics and Related Research, 58, pp. 249-270, 1968.

16. M. H. Shamos and L. S. Lavine, "Physical Bases for Bioelectric Effects in Mineralized Tissues," Clinical Orthopaedics and Related Research, 35, pp. 177-188, 1964.

17. E. Fukada and I. Yasuda, "Piezoelectric Effects in Collagen," Japanese Journal of Applied Physics, 3, pp. 117-121, 1964.

18. W. S. Williams and L. Breger, "Piezoelectricity in Tendon and Bone," The Journal of Biomechanics, 8, pp. 407-413, 1975.

19. C. A. Bassett, "Review: Biologic Significance of Piezoelectricity," Calcified Tissue Research, 1, pp. 252-272, 1968.

20. R. O. Becker, C. A. Bassett, and C. H. Bachman, "Bioelectrical Factors Controlling Bone Structure," Bone Biodynamics, Ed. by H. M. Frost, Little, Brown and Co., Boston, pp. 209-232, 1964.

21. R. O. Becker, "The Bioelectric Factors in Amphibian-Limb Regeneration," The Journal of Bone and Joint Surgery, 43-A, pp. 643-656, 1961.

22. R. J. Jendrucko, "Electrical Phenomena in Bone: Principles and Clinical Applications," Applied Physiological Mechanics, Ed. by D. N. Ghista, Harwood Academic Publishers, New York, pp. 181-229, 1979.

23. L. Breger, "Piezoelectricity in Bone and Tendon," Ph.D. Thesis, University of Illinois, Urbana, 1973.

24. S. Stephan, W. Swansen, and J. C. Mulier, "Experimental Study on the Electrical Impedence of Bone and the Effect of Direct Current on the Healing of Fractures," Clinical Orthopaedics and Related Research, 120, pp. 266-267, 1976.

25. M. H. Shamos and L. S. Lavine, "Piezoelectricity as a Fundamental Property of Biological Tissues," Nature, pp. 267-269, 1967.

26. J. V. Wait, L. P. Huelsman, and G. A. Korn, Introduction to Operational Amplifier Theory and Applications, Ed. by K. J. Bowman and M. Eichberg, McGraw-Hill, New York, 1975.

27. E. J. Kennedy, "A Study of the Theoretical and Practical Limitations of Low Current Amplification by Transistorized Current-Feedback D.C. Electrometers," Ph.D. Thesis, The University of Tennessee, Knoxville, 1967.

28. C. D. Motochenbacher and F. C. Fitchen, Low Noise Electronic Design, John Wiley and Sons, New York, 1973.

29. P. Z. Peebles, Probability, Random Variables, and Random Signal Principles, Ed. by S. W. Director, McGraw-Hill, New York, 1980.

30. B. K. F. Kummer, "Biomechanics of Bone," Biomechanics: Its Foundations and Objectives, Ed. by Y. C. Fung, N. Perrone and M. AnLiker, Prentice-Hall, Englewood Cliffs, New Jersey, p. 242, 1972.

31. G. V. B. Cochran, "Electromechanical Characteristics of Moist Bone," Ph.D. Thesis, Columbia University, New York, 1966.

APPENDICES

APPENDIX A

DATA FROM PROGRESSIVE LOADING EXPERIMENT

In this appendix the data which was obtained from the progressive loading experiment described in Chapter V is displayed. The signal was stored and plotted with a Hewlett-Packard Model 5420 A Digital Signal Analyzer and a Model 9872A Digital Plotter. The horizontal axis is in seconds and the vertical axis is in millivolts. A time delay was used in displaying the data so that the position of the neutral baseline could be approximated. The results obtained in this experiment are discussed in Chapters VI and VII.

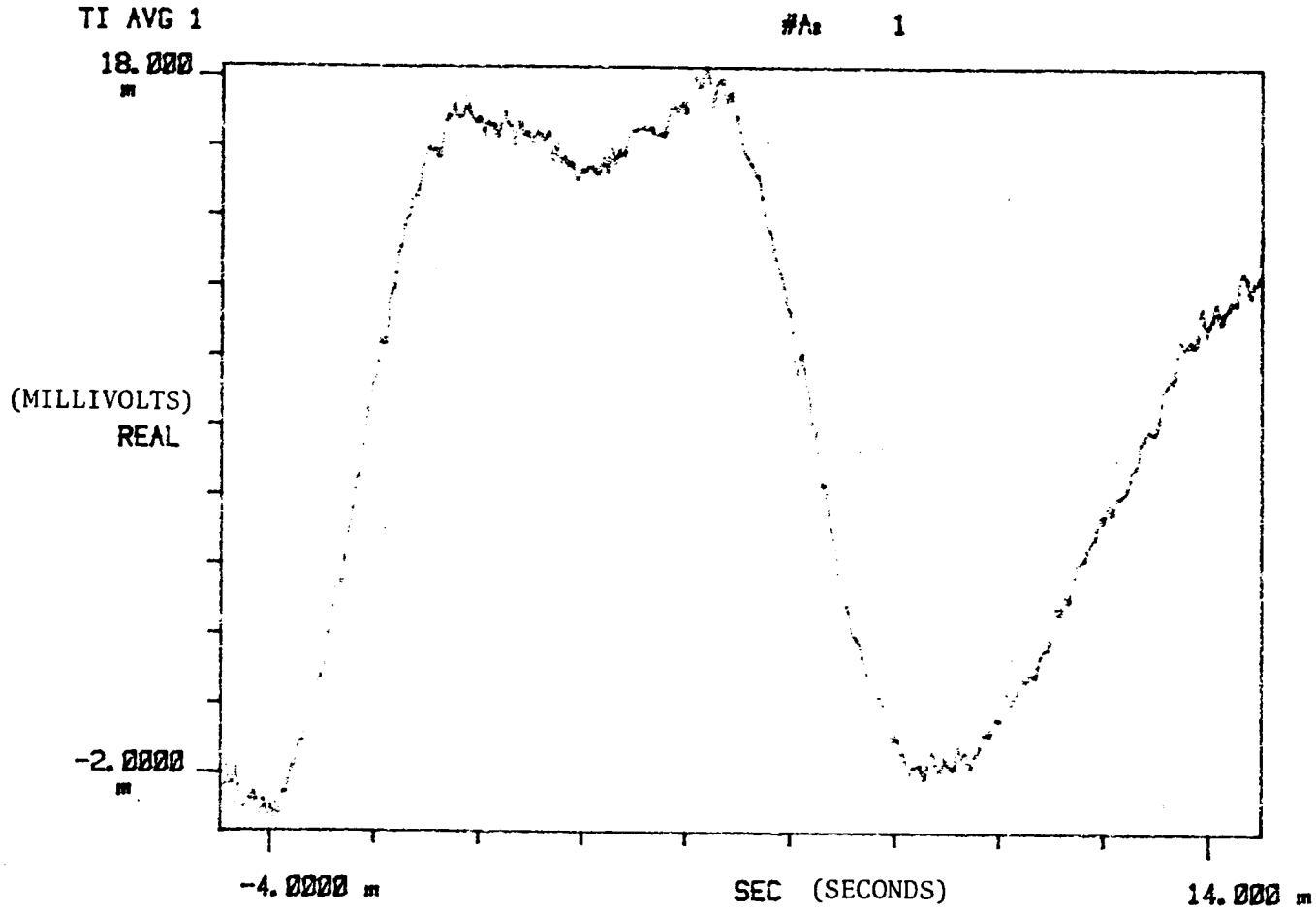

Figure 21. Current Waveform Obtained from Sample 10a Using a 1/16 Ounce Load.

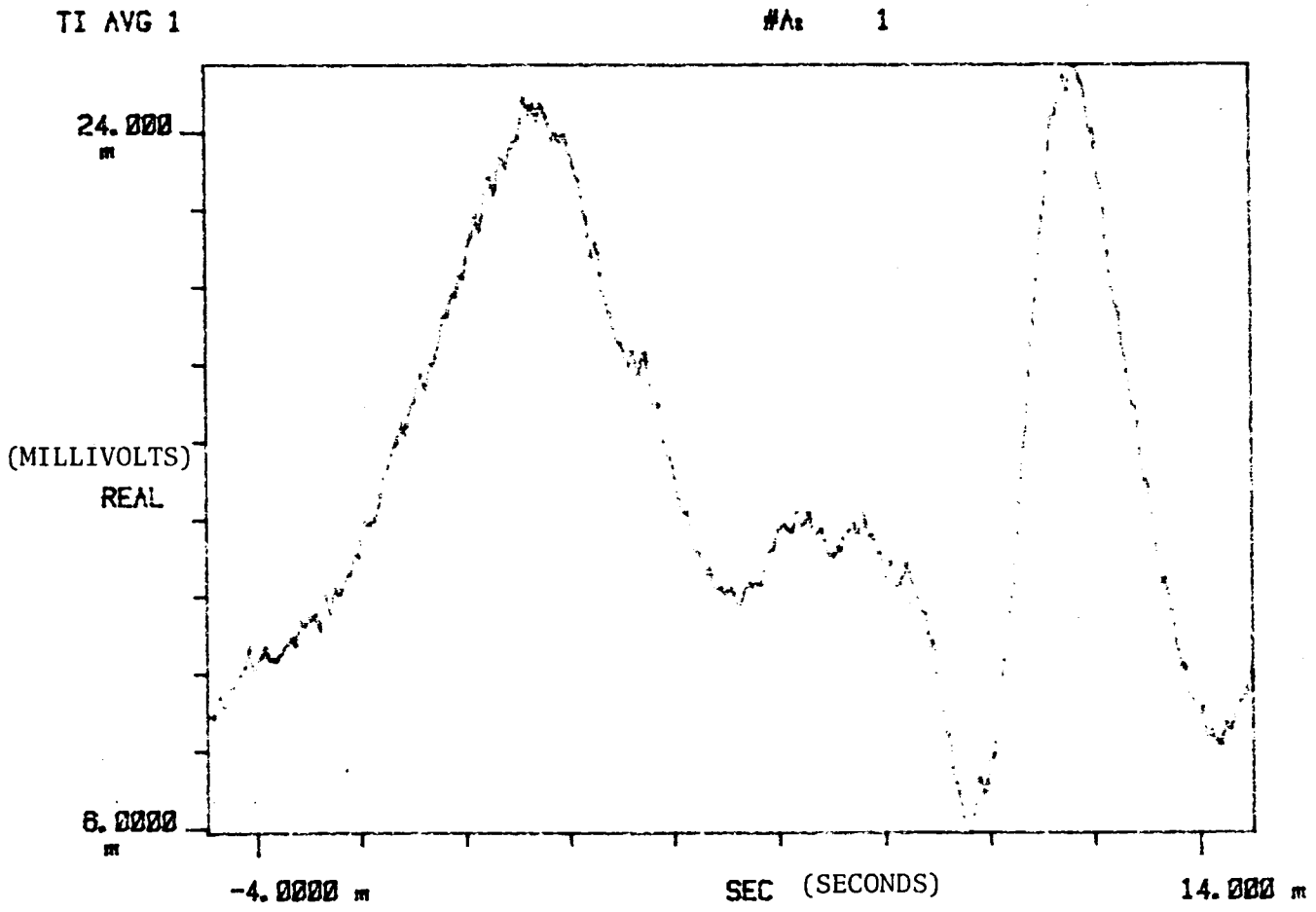

Figure 22. Current Waveform Obtained from Sample 10a Using a 1/8 Ounce Load.

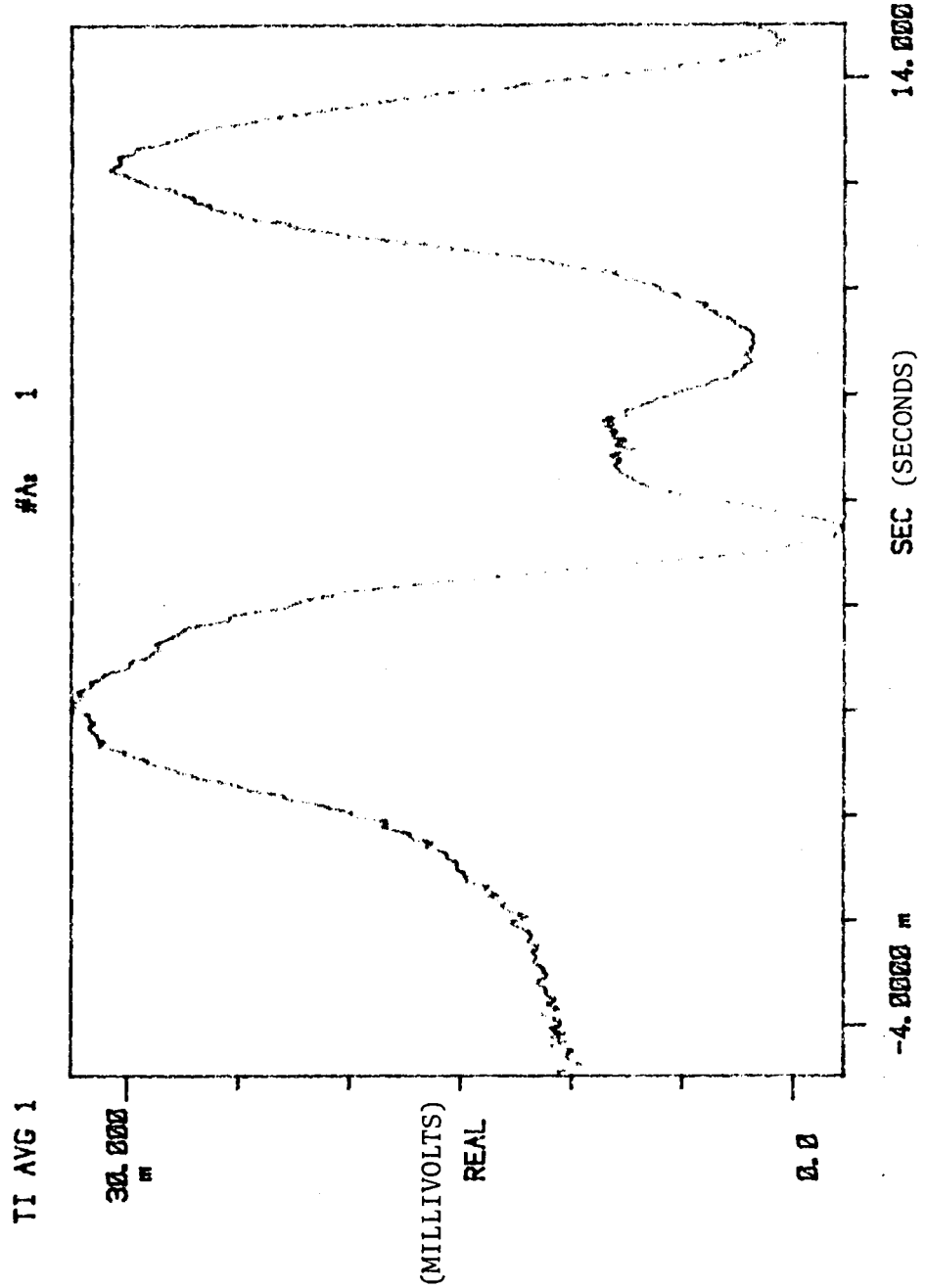

Figure 23. Current Waveform Obtained from Sample 10a Using a 1/4 Ounce Load.

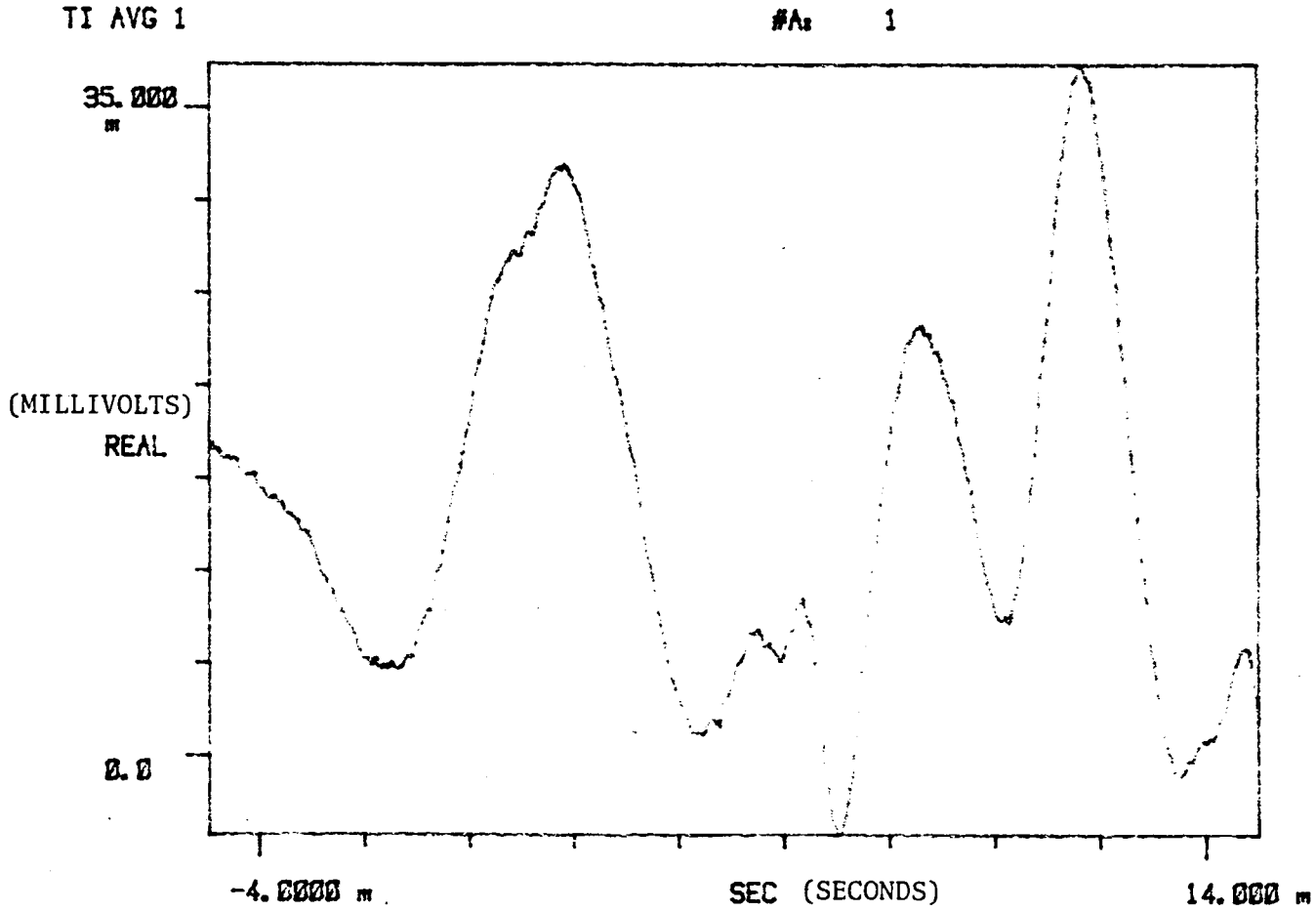

Figure 24. Current Waveform Obtained from Sample 10a Using a 1/2 Ounce Load.

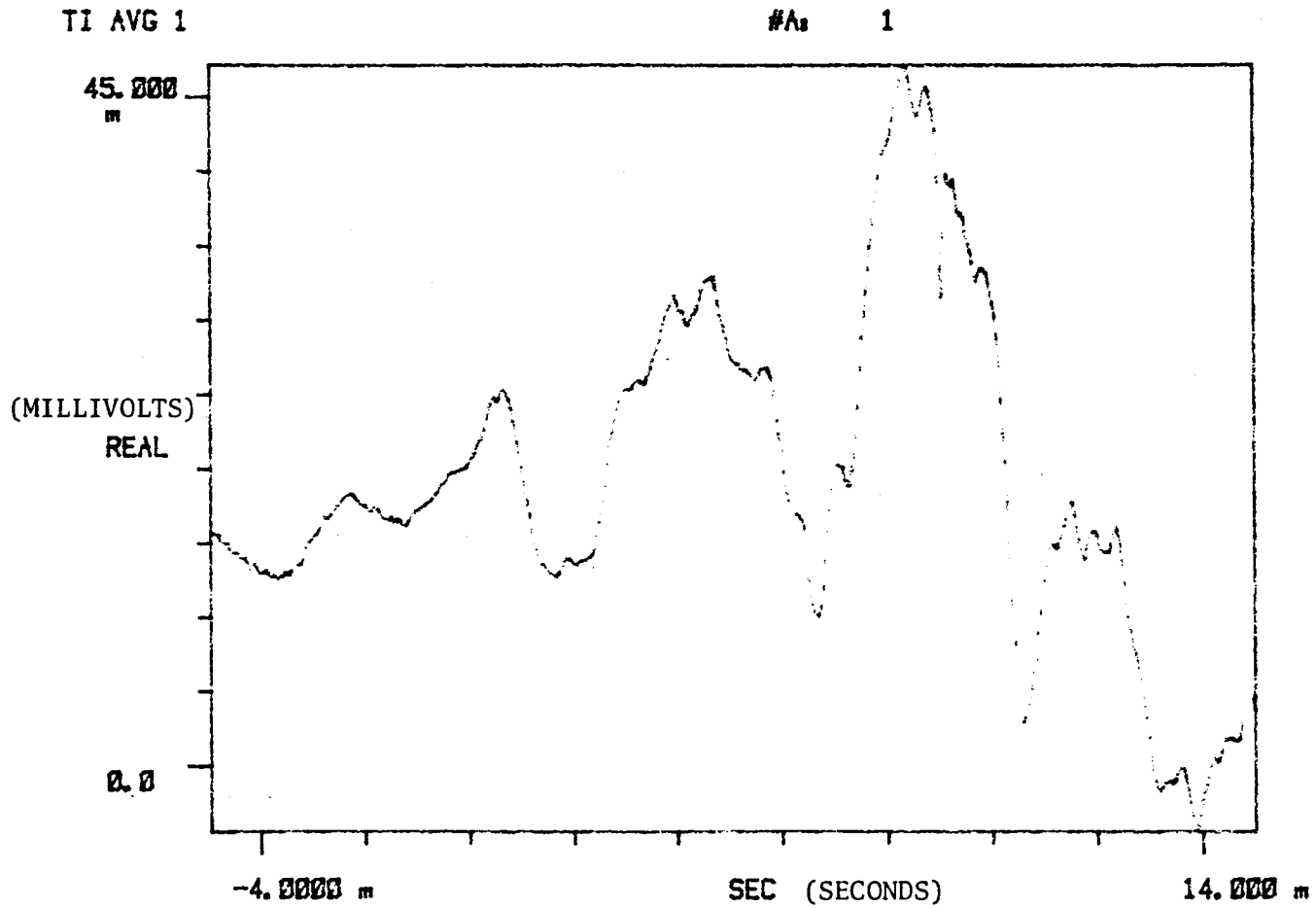

Figure 25. Current Waveform Obtained from Sample 10a Using a 1 Ounce Load.

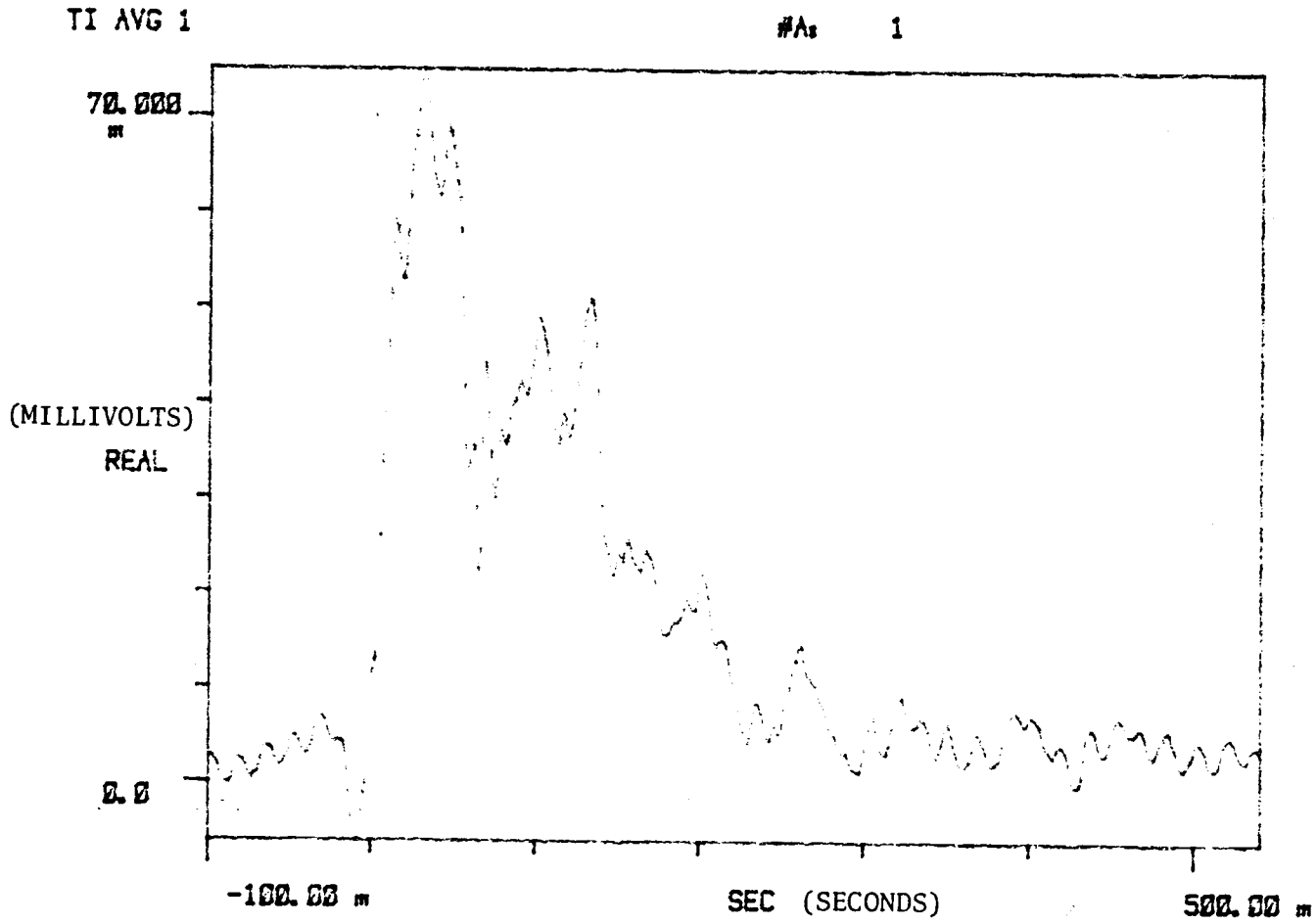

Figure 26. Voltage Waveform Obtained from Sample 5a Using a 1/16 Ounce Load.

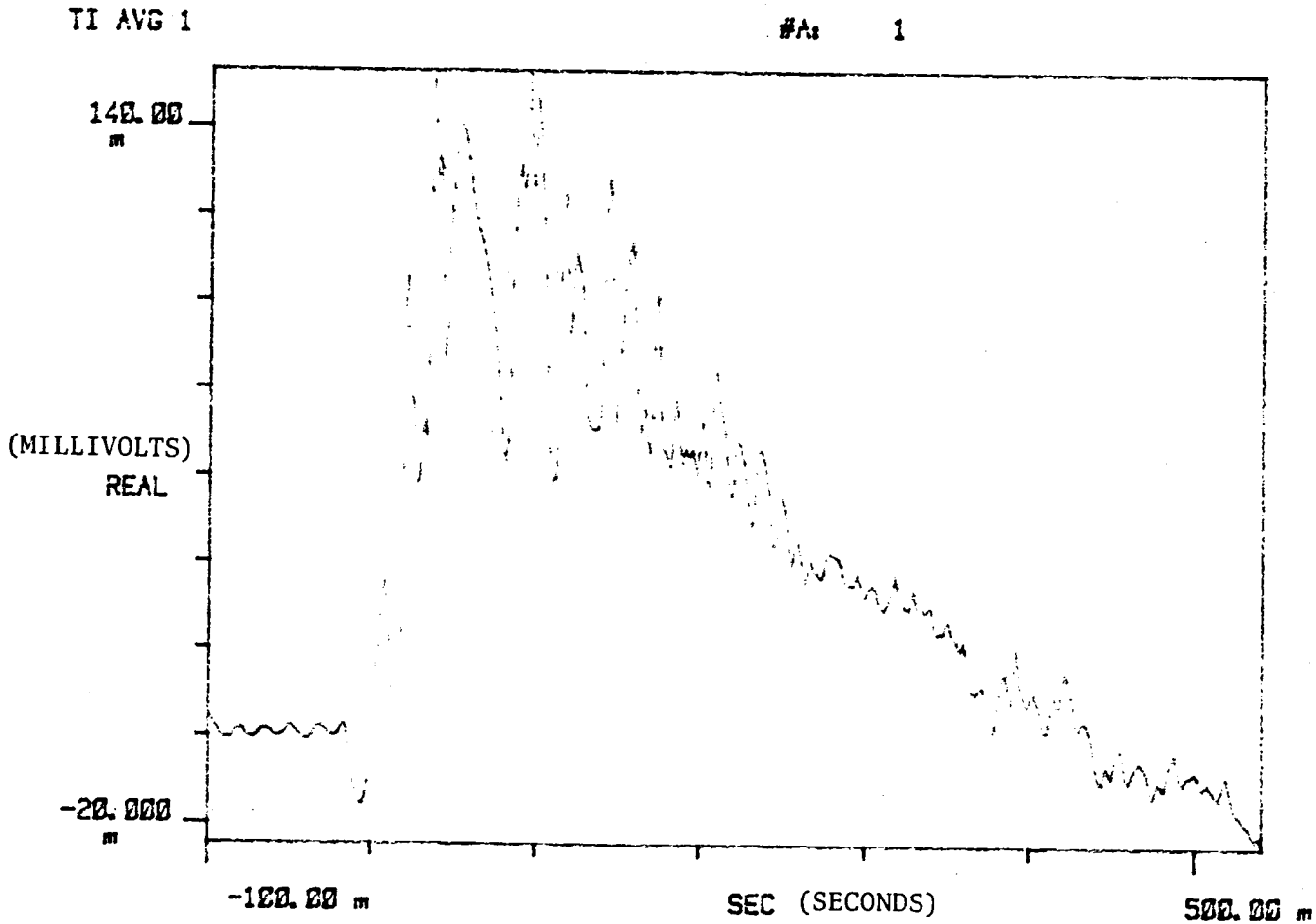

Figure 27. Voltage Waveform Obtained from Sample 5a Using a 1/8 Ounce Load.

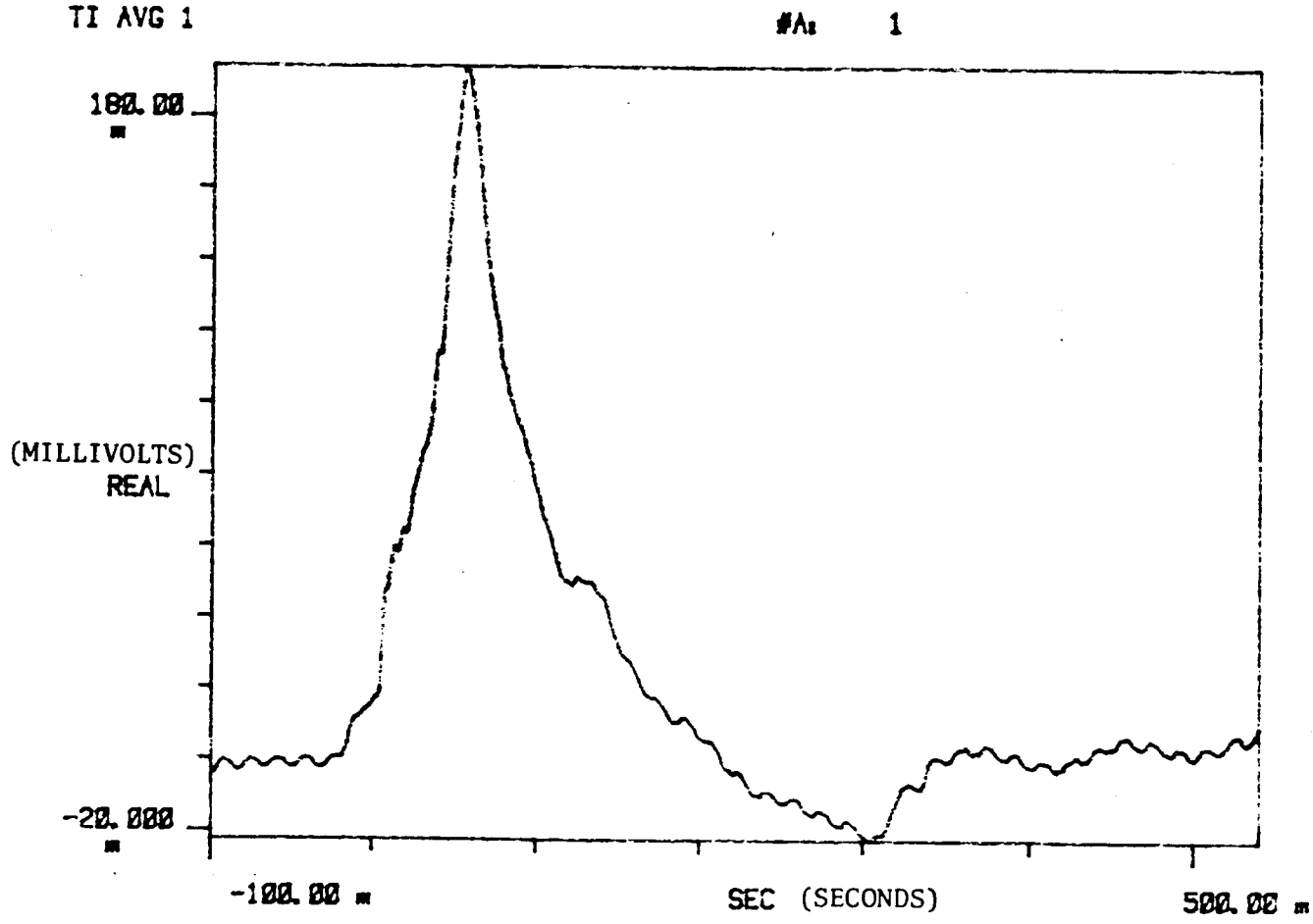

Figure 28. Voltage Waveform Obtained from Sample 5a Using a 1/4 Ounce Load.

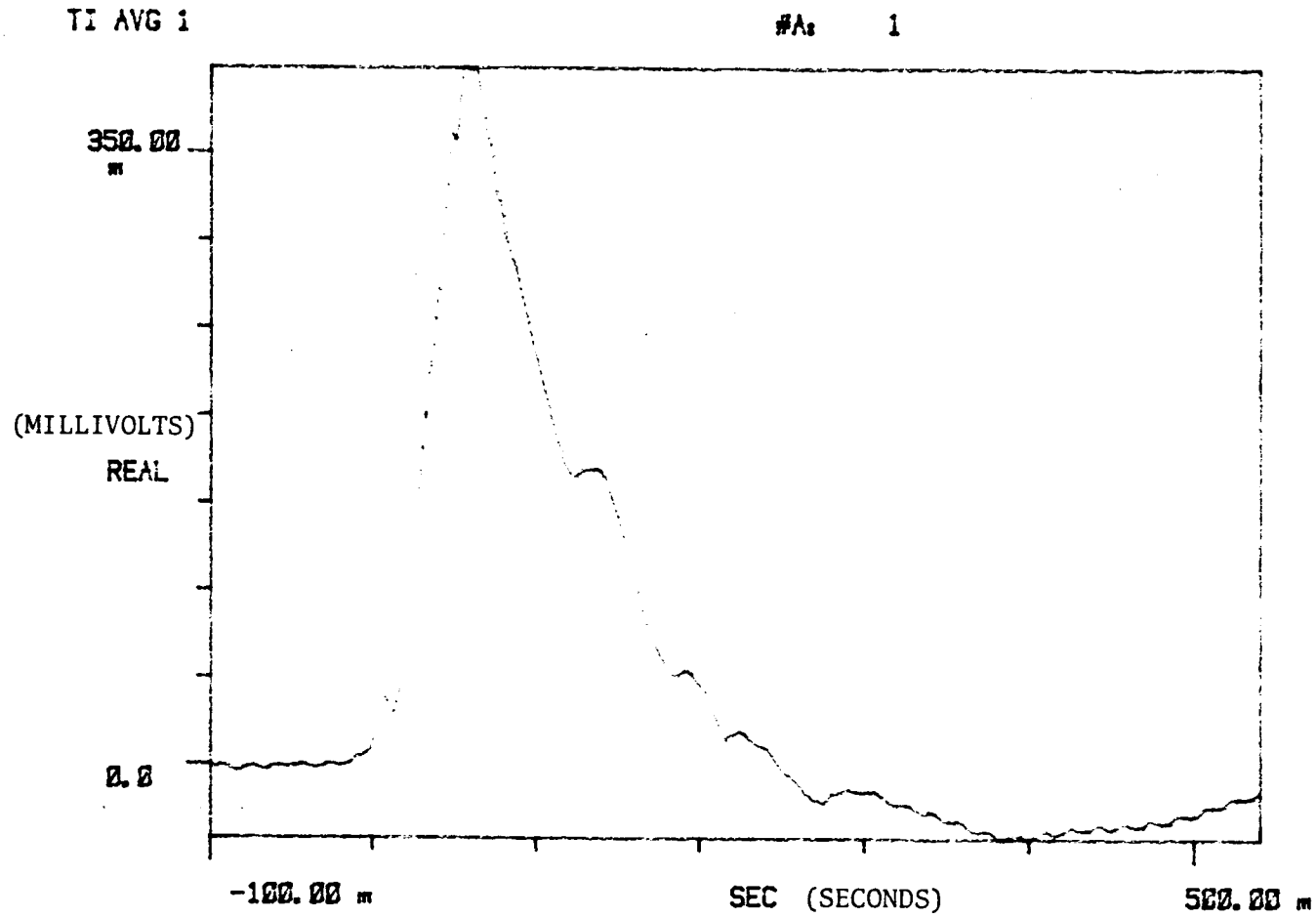

Figure 29. Voltage Waveform Obtained from Sample 5a Using a 1/2 Ounce Load.

APPENDIX B

DATA FROM THE FATIGUE LOADING EXPERIMENT

In this appendix the data generated as specimen 3x was loaded consecutively with a 1/2 ounce load is displayed. The transduction system was switched back and forth from the current to the voltage mode throughout the duration of this experiment in order to observe the effect of fatigue on both parameters. The signal was stored and plotted with a Hewlett-Packard Model 5420 A Digital Signal Analyzer and a Model 9872 A Digital Plotter. The top waveform in each figure represents the current and the bottom waveform represents the voltage generated in the mechanically stressed sample. The units of the horizontal axis is seconds and the vertical asix are in millivolts. The results of this experiment are discussed in Chapter VI.

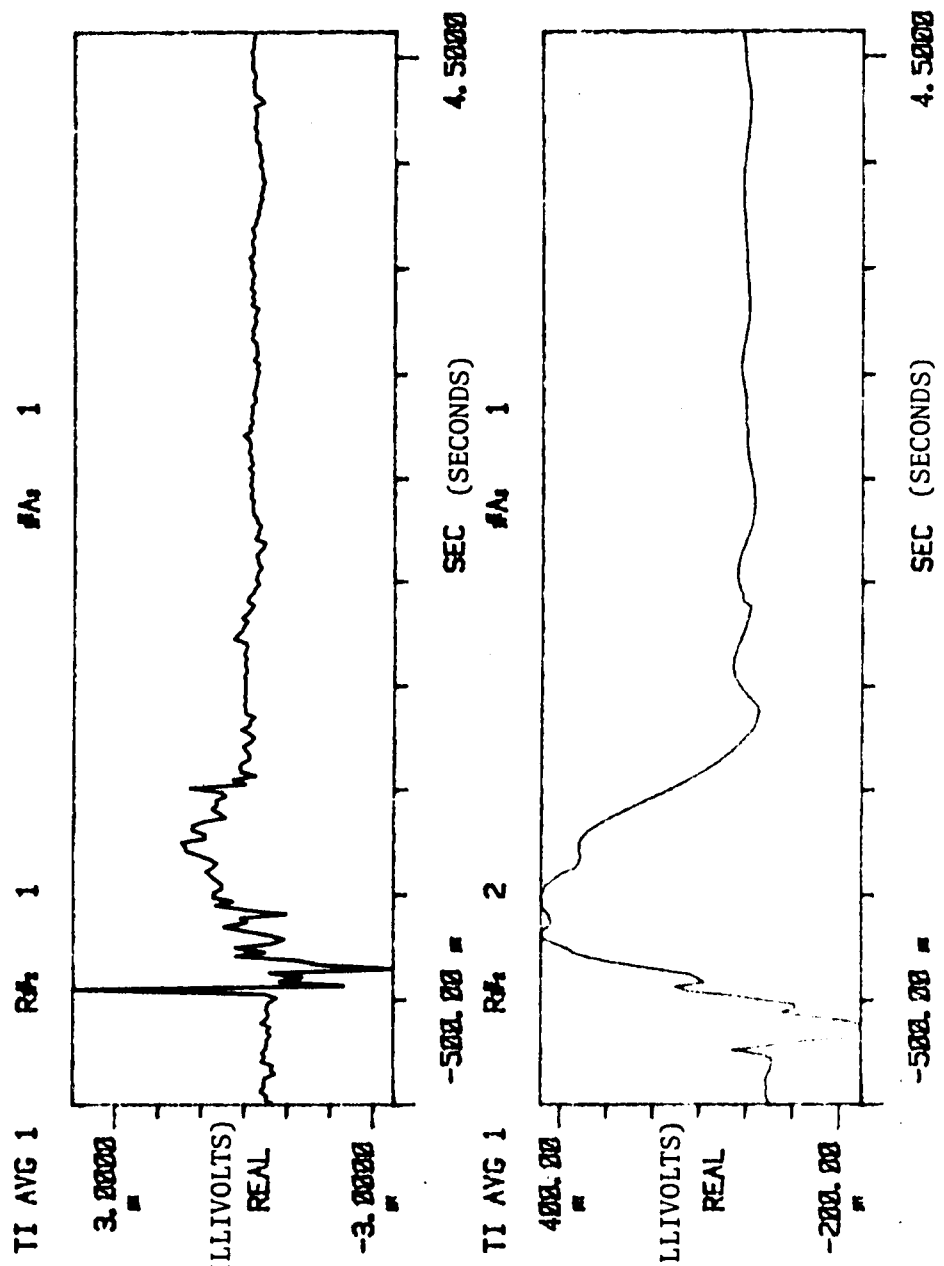

Figure 30. Data from First Loading.

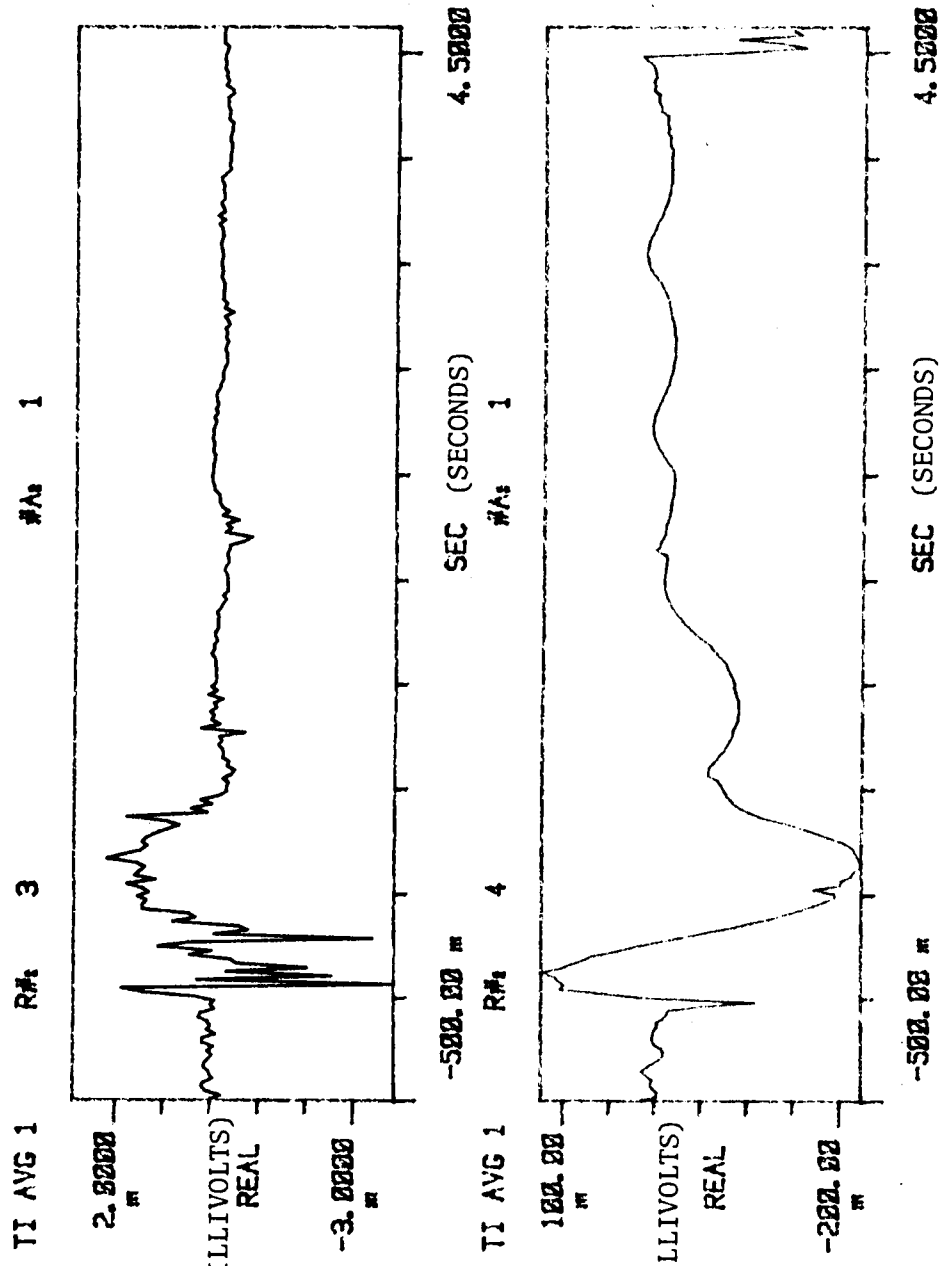

Figure 31. Data from Second Loading.

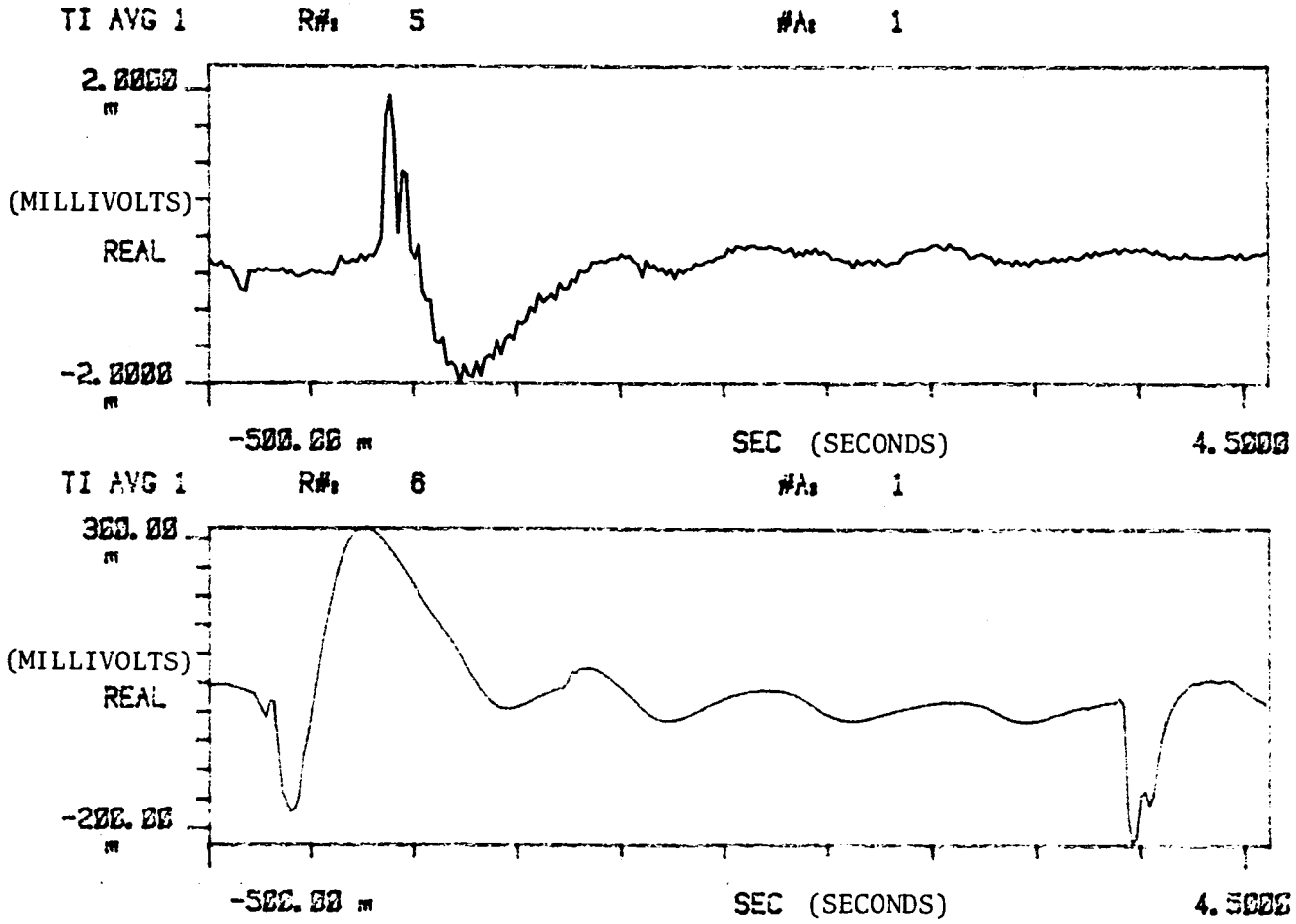

Figure 32. Data from Third Loading.

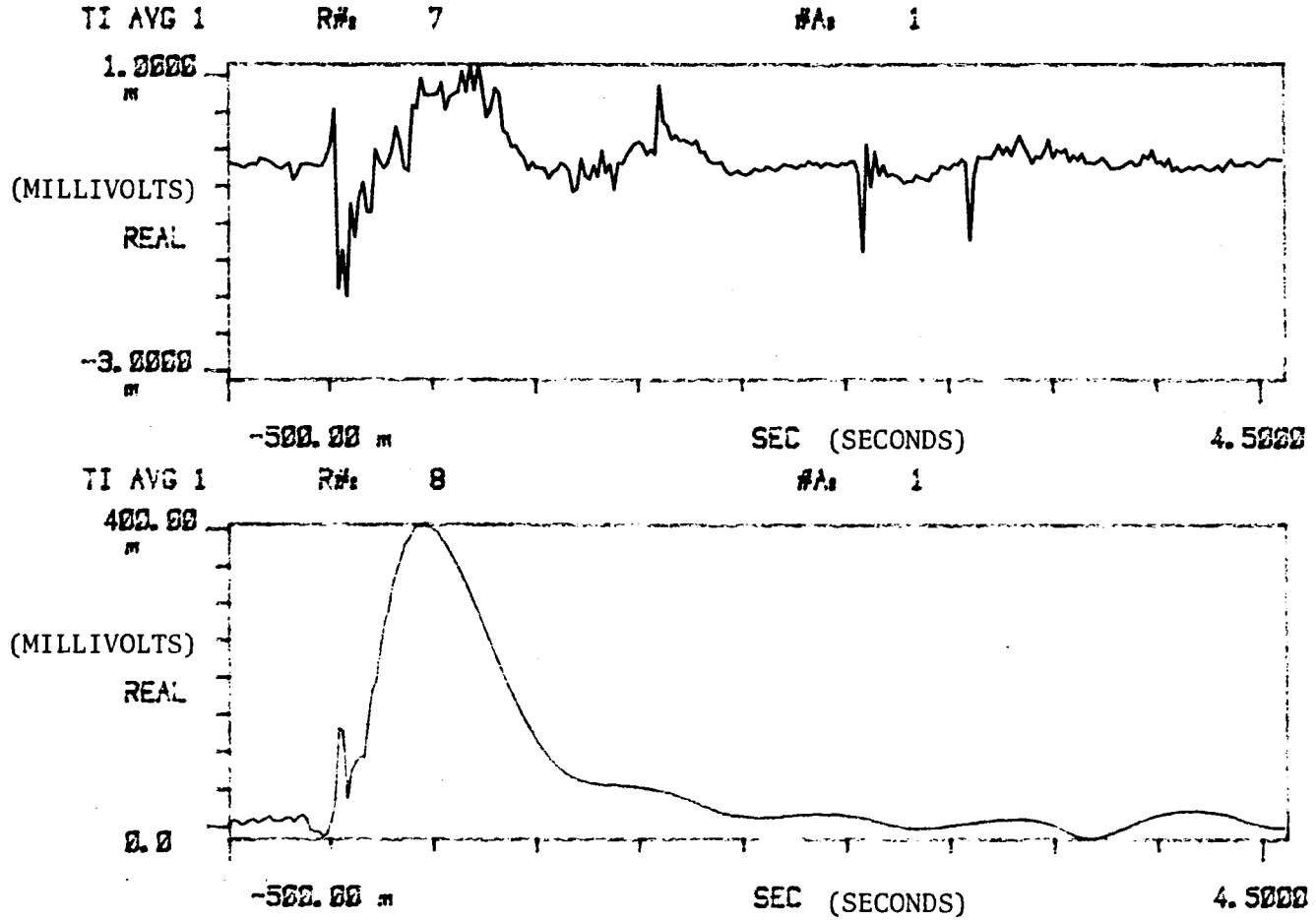

Figure 33. Data from Fourth Loading.

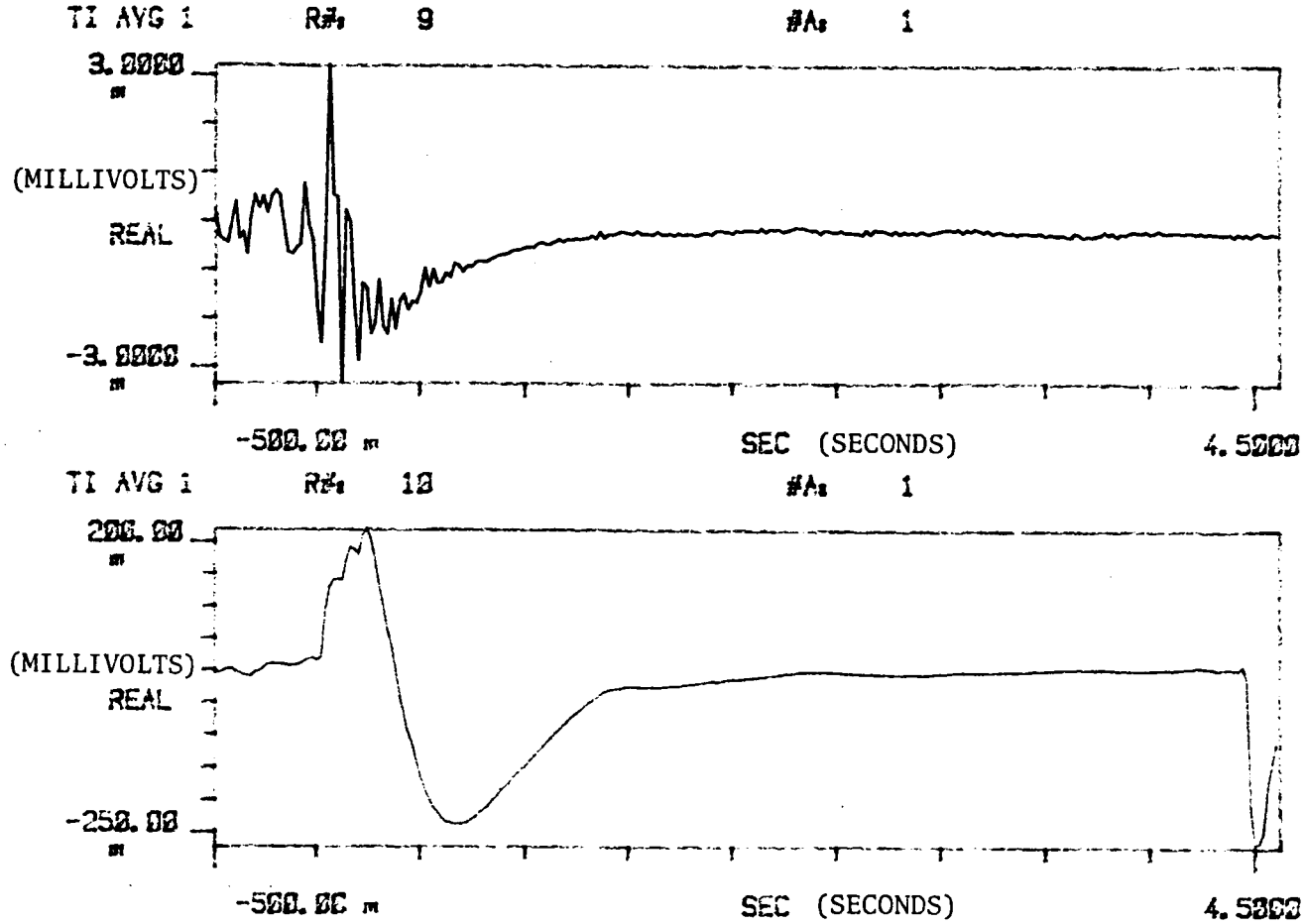

Figure 34. Data from Fifth Loading.

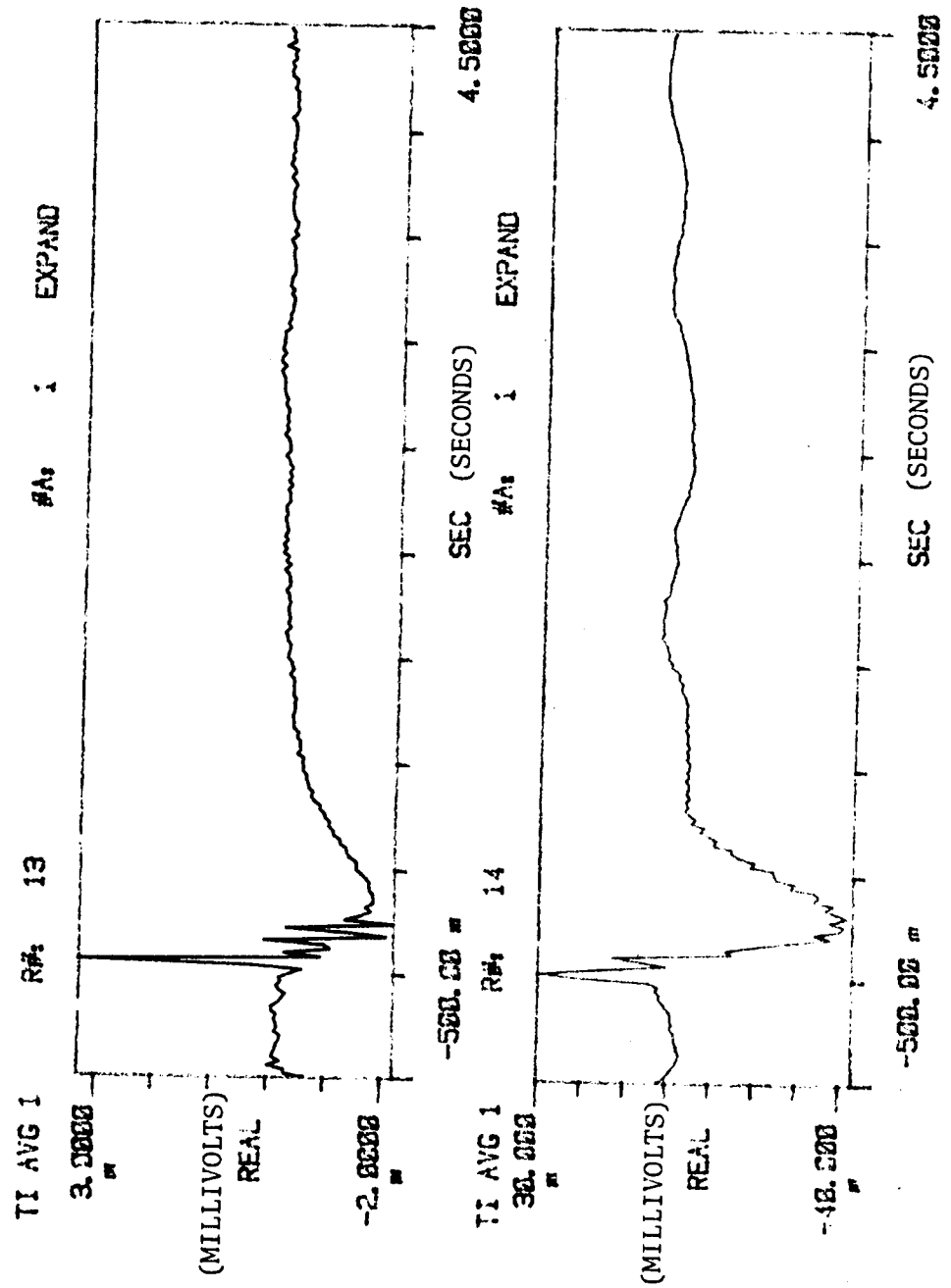

Figure 35. Data from Sixth Loading.

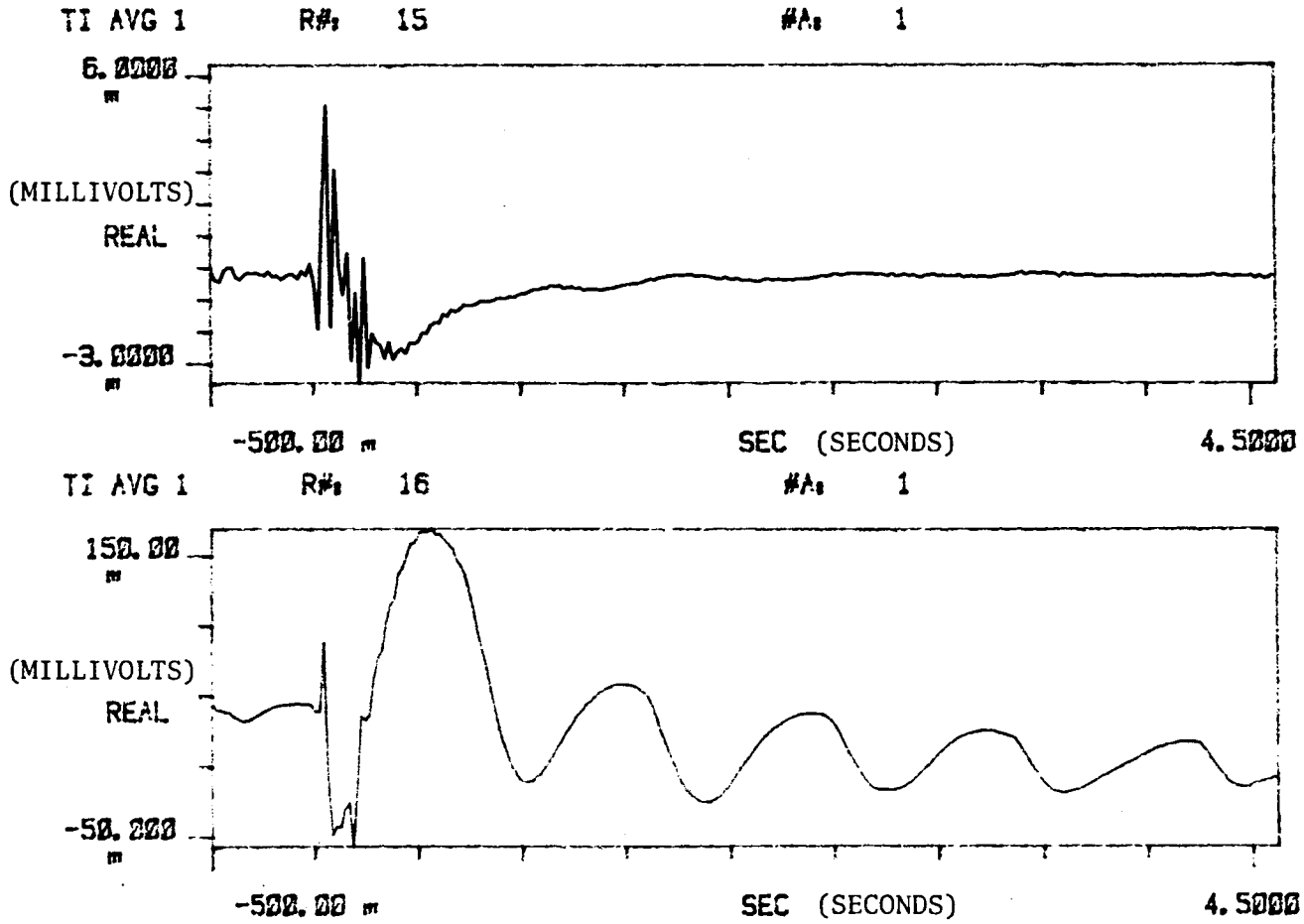

Figure 36. Data from Seventh Loading.

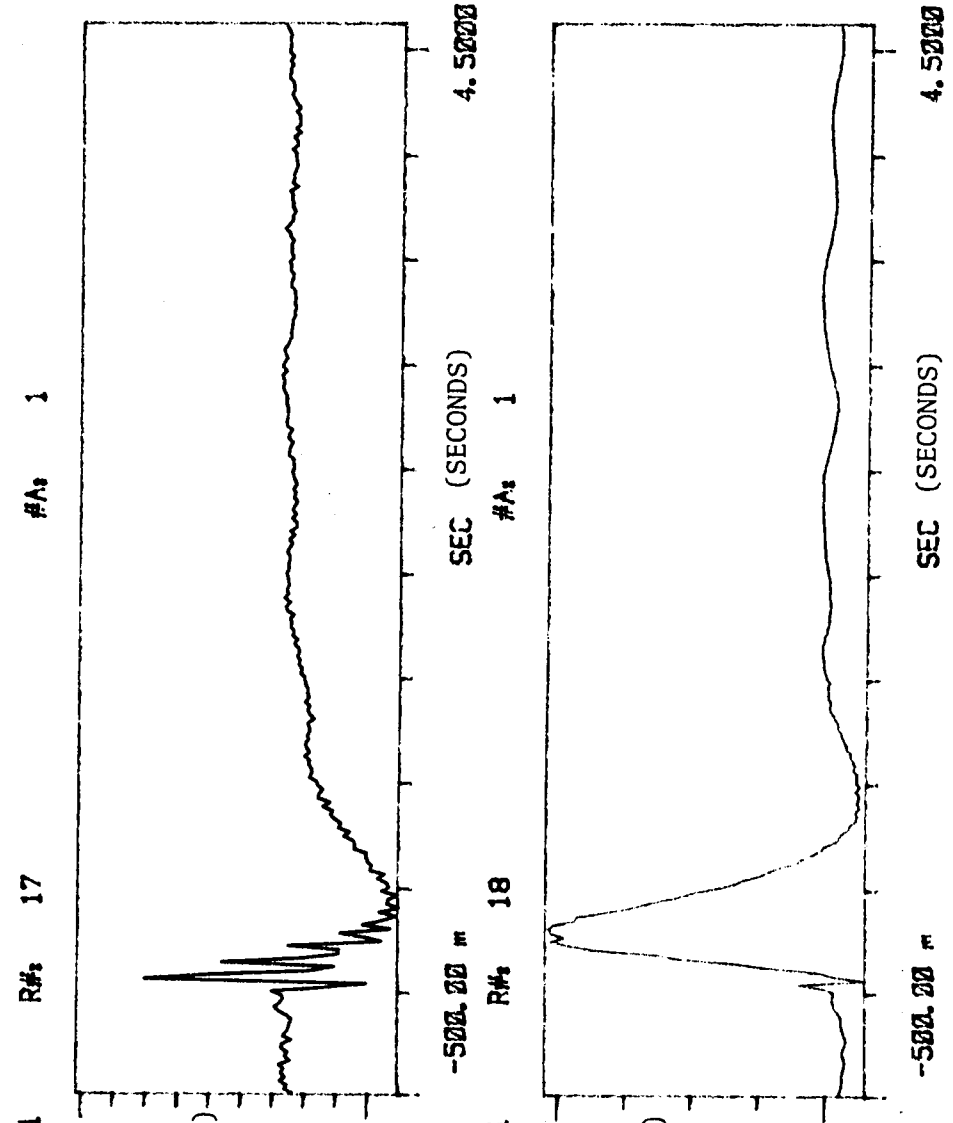

Figure 37. Data from Eighth Loading.

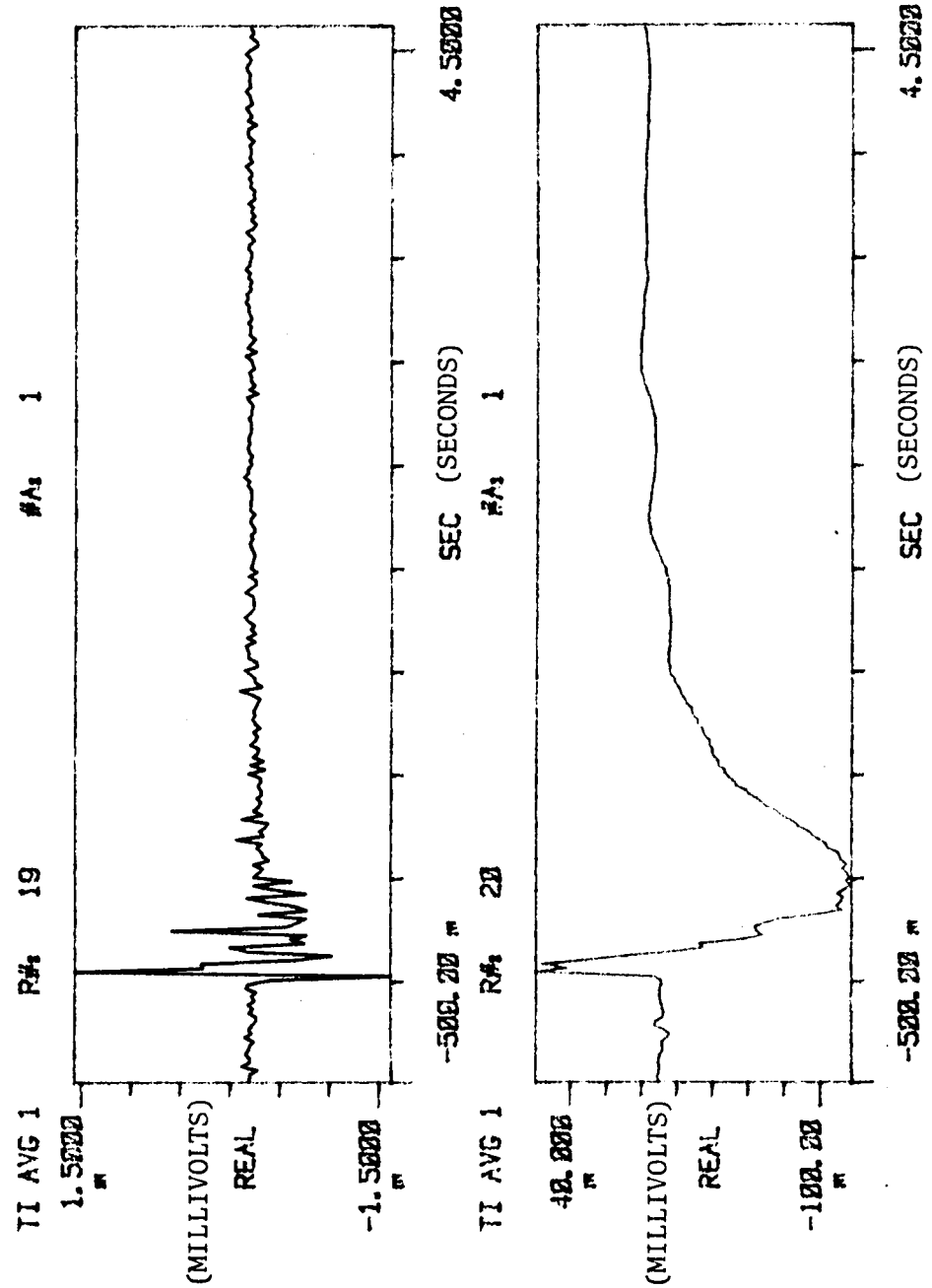

Figure 38. Data from Ninth Loading.

APPENDIX C

LIST OF SYMBOLS

A list of the symbols which were used in this work is presented here. The smaller case symbols are listed first, then the larger case symbols, and finally the Greek symbols.

a,b,c,d, e,f,g,h	Constants in F(s).
d_{ij}	Piezoelectric Moduli.
f	Stress Gradient Piezoelectric Moduli.
f_{hi}	Frequency Region of White Noise.
f_2 - f_1	Roots of the Characteristic Equation of G(s).
r_1, r_2, r_3	Roots of the Characteristic Equation of G(s).
A_o	Magnitude of Open Loop Gain.
A_v	Open Loop Gain.
C_f	Feedback Capacitor.
C_g	Source Capacitance.
C_1	Input Capacitance.
$\overline{E_g^2}$	Thermal Noise Generated by R_g.
$\overline{E_n^2}$	Equivalent Input Noise Voltage of the Amplifier.
$\overline{E_{ni}^2}$	Equivalent Input Noise.
$\overline{E_{no}^2}$	Equivalent Ouput Noise.
$\overline{E_{noI}^2}$	Output Noise Due to the Input Noise Current.
$\overline{E_{noT}^2}$	Output Noise Due to the Thermal Effects.
$\overline{E_{noV}^2}$	Output Noise Due to the Input Noise Voltage.

Moment resisting

General Height
2 story Building

$\overline{E_{Rf}^2}$	Thermal Noise Generated by R_f.
$\overline{E_{R2}^2}$	Thermal Noise Generated by R_2.
$\overline{E_{R3}^2}$	Thermal Noise Generated by R_3.
$E(t)$	Electric Field Resulting from Stress.
$F(s)$	General Transfer Function.
$F(t)$	Applied Load in Bone.
$G(s)$	Output Due to a Step Input.
$G(t)$	Inverse Laplace of G(s).
G_1	Transfer Function $\frac{\sigma_1(t)}{F(t)}$.
G_2	Transfer Function $\frac{E(t)}{\sigma_1(t) - \sigma_2(t)}$.
H	Transfer Function $\frac{\sigma_2(t)}{E(t)}$.
$\overline{I_n^2}$	Equivalent Input Noise Current of the Amplifer.
$\overline{I_{ni}^2}$	Equivalent Input Noise Current.
I_1	Input Current.
K	Boltzmann's Constant
$N(\omega)$	Power Spectral Density.
P_i	Polarization Vector
R_B	Bias Resistor.
R_f	Feedback Resistor.
R_g	Source Resistance.
R_L	Load Resistor.
R_o	Output Resistance.
R_1	Input Resistance.
R_2	Feedback Resistor.
R_3	Feedback Resistor.

T	Absolute Temperature.
$T(j\omega) \cdot T(-j\omega)$	Power Transfer Function.
V_1	Input Voltage.
$V_1 - V_2$	Differential Voltage.
V_o	Output Voltage.
Z_f	R_f in parallel with C_f.
Z_g	R_g in parallel with C_g.
Z_1	R_1 in parallel with C_1.
$\alpha,\beta,\gamma,\delta$	Constants in G(t).
$\frac{\partial\sigma}{\partial x}$	Stress Gradient.
σ_{ij}	Stress Tensor.
$\sigma_1(t)$	Stress Resulting from an Applied Load.
$\sigma_2(t)$	Stress Resulting from Oriented Bone Growth.
τ_r	Rise Time.
ω_o	-3dB Radian Frequency.

VITA

Marcus Livingstone Simpson was born on November 18, 1952, in Memphis, Tennessee. He attended elementary school and junior high in Maryville, Tennessee, and then transferred to Webb School of Knoxville, Tennessee, where he received his high school diploma in June 1971. In September of 1971 he entered Trinity University in San Antonio, Texas, and was awarded the Bachelor of Science degree in Biophysics in December 1975. In September of 1976 he began work on a second B.S. in The University of Tennessee's Department of Engineering Science and Mechanics. In September of 1977 he was admitted to a Master's program in the same department and thus worked concurrently on two degrees. He was awarded the Bachelor of Science degree in Engineering Science and Mechanics in March 1980 and is expected to receive the Master of Science degree in August 1980.

The author is a member of the Blue Key Honor fraternity and a member of the I.E.E.E. Instrumentation and Biomedical groups. He is active in church and in community activities like scouting. He enjoys most sports including golf, tennis, and softball, and in college played on the Trinity University soccer team. His hobbies include playing the banjo, bicycling, and backpacking.